SKB

TECHNICAL REPORT 91-30

A resistance network model for radionuclide transport into the near field surrounding a repository for nuclear waste (SKB, Near Field Model 91)

Lennart Nilsson, Luis Moreno, Ivars Neretnieks,
Leonardo Romero

Department of Chemical Engineering,
Royal Institute of Technology, Stockholm

June 1991

SVENSK KÄRNBRÄNSLEHANTERING AB
SWEDISH NUCLEAR FUEL AND WASTE MANAGEMENT CO

BOX 5864 S-102 48 STOCKHOLM

TEL 08-665 28 00 TELEX 13108 SKB S
TELEFAX 08-661 57 19

A RESISTANCE NETWORK MODEL FOR RADIONUCLIDE TRANSPORT INTO THE NEAR FIELD SURROUNDING A REPOSITORY FOR NUCLEAR WASTE (SKB, NEAR FIELD MODEL 91)

Lennart Nilsson, Luis Moreno, Ivars Neretnieks,
Leonardo Romero

Department of Chemical Engineering,
Royal Institute of Technology, Stockholm

June 1991

A RESISTANCE NETWORK MODEL FOR RADIONUCLIDE TRANSPORT INTO THE NEAR FIELD SURROUNDING A REPOSITORY FOR NUCLEAR WASTE (SKB, Near Field Model 91)

Lennart Nilson, Luis Moreno, Ivars Neretnieks, Leonardo Romero
Department of Chemical Engineering
Royal Institute of Technology
S-100 44 Stockholm, Sweden.

June 1991

KAT 91/12

ABSTRACT

A model has been developed, describing the steady state transport of dissolving species of radionuclides from a single canister in a repository for spent nuclear fuel out into the passing water in fractures in the surrounding rock matrix. The transport of nuclides is described by a network of transport resistances, coupled together in the same way as an electrical circuit network. With the model a number of calculations are done for various sets of fracture geometry data. The calculations indicate that the resistance network model gives results comparable to those of a complex 3-dimensional numerical model.

SUMMARY

In this report a model is developed, describing the steady state transport of dissolving species of radionuclides from a single canister in a repository for spent nuclear fuel out into the passing water in fractures in the surrounding rock matrix.

The transport of nuclides is described by a network of transport resistances, coupled together in the same way as an electrical circuit network.

The model is developed in steps, where the initial basic network describes transport from a completely corroded canister, through a backfill of compacted bentonite clay, surrounding the canister and into a fracture intersecting the repository hole. It is assumed that the backfill clay will penetrate a short distance into the fracture. From the backfill nuclides enter the fracture via a number of transport routes leading directly into the fracture mouth or through the rock matrix.

This basic network model is subsequently expanded to cover other types of damage to the canister, fabrication damage or localized corrosion resulting in a hole of limited size in the canister wall and shearing of the canister resulting in a fracture in the canister wall. To the model is also added a transport route leading to the so called "disturbed zone" around the transport tunnel in which the repository is located.

With the model, calculations are done for a number of different data sets in which the fracture geometry is varied around a central case in which fractures with a aperture of 0.1 mm are spaced at 1 m between each and with backfill penetrating 1 cm into the fracture mouth.

In the cases with localized damage to the canister it is assumed that the hole in the canister or the wall fractures are situated directly opposite to a fracture in the rock.

The calculations for the central case are compared to results obtained for the same case in a 3-dimensional numerical model. The results show a very good agreement between the two models indicating that the easy to use resistance network model will give sufficiently accurate results. It is also shown that the proposed approach gives a model that is easily expanded to more complex transport scenarios, still retaining a very simple system of linear equations.

TABLE OF CONTENTS

1 INTRODUCTION AND BACKGROUND

The present report describes a model for steady state field transport. It is an extension to the model used in KBS-3 (1983). The underlying concept is based on the transport by diffusion of dissolving species of radionuclides from a single canister in a repository for spent nuclear fuel out into the passing water in the fractures. Only transport by diffusion is considered in this model since the hydraulic conductivity of the backfill is very small. It has been shown earlier that the advective transport in the backfill de facto is negligible compared to the transport by diffusion.

In the initial model nuclide transport is described by the resistances to the mass transfer of radionuclides

* by diffusion through the backfill of compacted bentonite
* by diffusion through the rock matrix
* by diffusion through a plug of backfill penetrating into the fracture
* by diffusion through a plug of stagnant water in the fracture
* transfer into a channel of flowing water in the fracture - the width of the channel varying from w=0.1 to 9 m and with a water velocity of $u_F=\varepsilon' \cdot u_0$. ε' being the effective flow porosity, and u_0 the superficial water velocity in the system.

In order to simulate the overall transport the resistances are coupled in a resistance network.

Figure 1 shows a simplified view of the transport paths. A nuclide that dissolves at the fuel's surface will diffuse out through the water in the gap between the fuel pellet and the zircaloy tube. The gap may eventually fill with corrosion products formed by the oxidation of the fuel and the zircaloy. The species then proceeds to diffuse out through the hole in the copper canister and further out through the backfill. Some of the species diffuse into the rock surrounding the backfill, some goes through the fractures which intersect the hole and some will diffuse upward to the backfill in the tunnel above. The fraction of the species taking the different routes depends on the relative resistances. At early times after breakthrough of the canister there is an instationary buildup of the concentration profile in the backfill and in the rock. For nonsorbing species it will only have a short duration in the order of tens of years in the backfill. In the rock the buildup can take much longer but it is difficult to assess the time since the extent of the rock is not known.

The transport route to the flowing water in the fracture will depend on the location of the fracture and on how it intersects the repository hole. It may also be noted that there may be one, two or more fractures intersecting a particular hole.

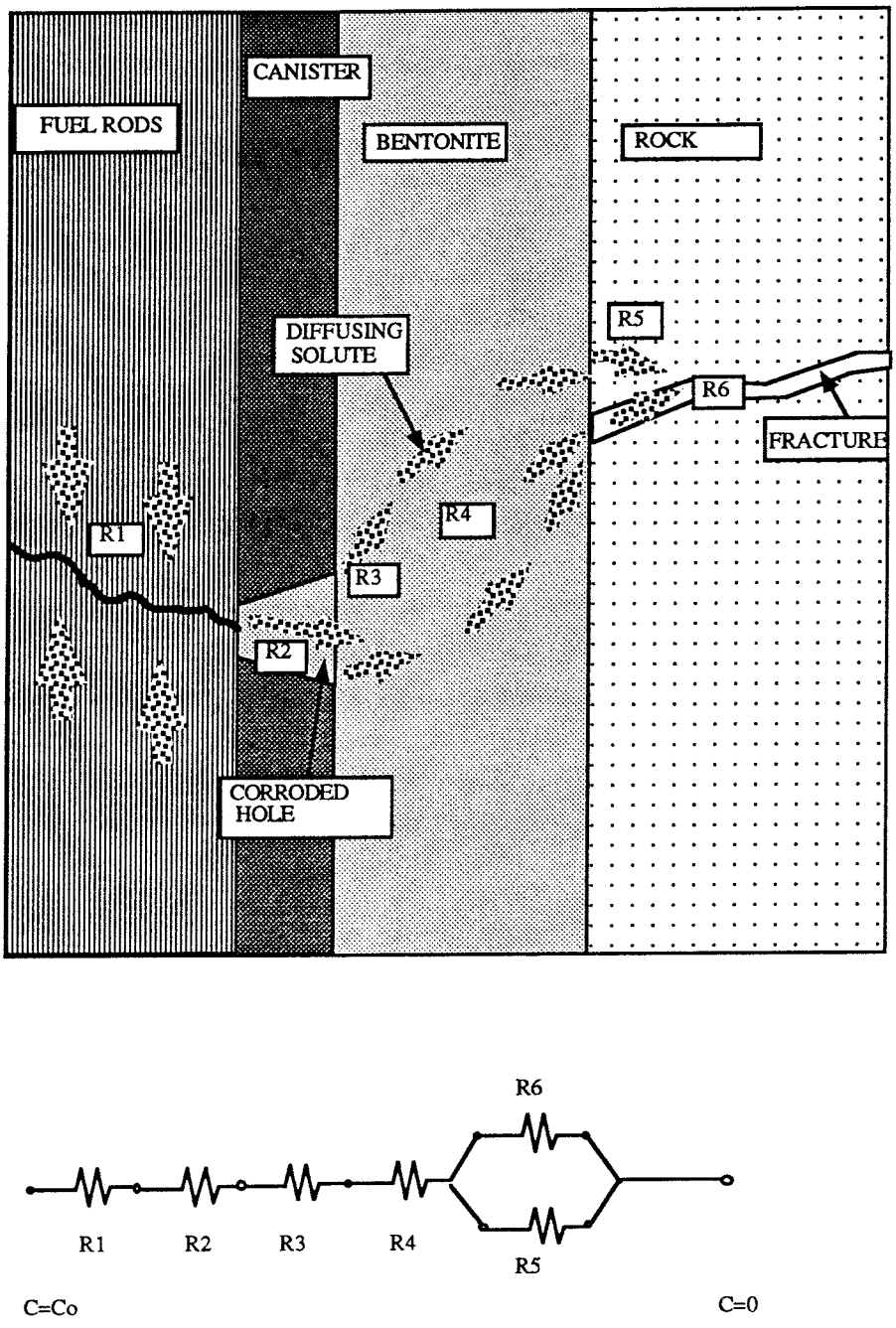

Figure 1. Simplified view of the transport paths.

There is no simple mathematical model that fully can handle this complex situation. There are several models that describe the transport in the different pathways independently. There are also some models that couple some of the pathways in the same model. In order to use the models independently one needs to know the boundary conditions and as these depend on the other models one must in principle solve all the part models simultaneously. We do it in the present model by adding resistances in the same manner as one does it for an electrical circuit. This leads to a very simple concept and also to a very compact and transparent model.

There are of course obvious drawbacks using this approach because it is necessary to simplify the system. In the real system the geometry is complex and the pathways are not independent of each other. The intersecting fracture with its channel(s) may intersect at any angle and be in any location relative to the canister. The channel is not an even slit but has a variable aperture and variable flowrates locally. The rock transport properties are also variable and the fracture may be filled by clay to some distance from the hole. Due to the variability of these and other properties it does not seem warranted to use an "exact" geometric description of each canister. It seems more adequate to make some simplifying generalizations and to accept that some errors will be introduced by the simplifications. It seems reasonable to assume that it would not be possible to obtain such a detailed knowledge of the data needed for a "full" description anyway that a more sophisticated model would be of use. Instead we have chosen to proceed in a stepwise manner, developing and testing the submodels in various ways.

2 GEOMETRIC MODEL

The canister (radius = r_1 m) is held in a repository hole with the radius r_2 m. The annulus between the canister and the perimeter of the hole is filled with a backfill consisting of bentonite clay. In the models the canister is considered as infinitely long (end effects are disregarded)

The rock matrix is fractured by parallel fractures at equal distances (s m between each fracture). The fractures intersect the repository hole perpendicular to the canister axis. The fractures are assumed to have an average width of δ m.

Clay from the repository hole may penetrate into the fracture to a distance of σ m.

Since a number of planes of symmetry can be identified, see figure 2, the geometry of the system can be simplified. Thus if we consider the case where a channel of limited width (w m) "hits" a canister, the canister will divide the channel in two parts, that can either be of equal size or distributed with the fraction ζ to one side and $(1-\zeta)$ to the other, each flowing along one side of the canister with a contact length of $\pi \cdot r_2$ before they merge again downstream of the canister. Each half of the canister together with the part of the channel passing it can be treated separately. The fracture in which the channel is running is of equal width in the entire nearfield surrounding the canister. (figure 2)

2.1 Submodels

2.1.1 Transport along the gap inside the zircaloy tubes

In a canister that has been penetrated the zircaloy tubes must also be breached for the nuclides to diffuse out. The general corrosion rate of zircaloy can be assumed to be very low. It is possible that the tubes still are mostly intact and that the nuclides must diffuse in the narrow gap between the tube and the fuel pellets. The gap may also be filled with corrosion products of either zircaloy or uranium oxide in a higher oxidation state. The diffusion resistance in the gap is very large and unless the uranium itself diffuses away to a large extent the rate of movement by diffusion will be low in the tube. Also it is difficult to conceive how most of the mass in the tube would disappear without something else filling in the void either as corrosion products or by mechanical creep.

Also if the zircaloy would corrode the escaping nuclides would have to move a long distance through the corrosion products in order to reach the hole in the canister.

There are so many possible cases which one could consider including the effects of partial dissolution of the uranium oxide and so many dubious assumptions one would have to make that we have elected at present no to address this problem. Instead we assume that there is no transport resistance inside the degraded canister. This certainly overestimates the release rate.

2.1.2 Transport through the canister wall

The damage to the canister can be of different types and extent, namely

1. the entire canister wall is assumed to be completely corroded, resulting in a free release of dissolved nuclides from the entire canister surface.
2. localized corrosion resulting in a hole of limited size in the canister wall.
3. a canister fracture, either caused by shearing of the canister, e.g. during an earth quake, or through a construction error, resulting in a fracture of limited width extending around the entire canister perimeter.

For the initial scenario for modelling the release of nuclides, the damage to the canister is assumed to be of the first type.

This model is then extended to cover also damages according to type 2, a circular hole of limited diameter in the canister wall as well as type 3, a slit in the canister, with uniform aperture around the entire canister.

2.1.3 Transport in the backfill

The transport in the backfill is by diffusion and Fick's law is directly applicable. The basic model is based on the case of radial diffusion from a totally degraded canister to the rock surface. For the case where the rock is assumed to be impermeable except for the fracture which intersects the hole at a known location an analytical solution was found (Neretnieks, 1983)

The transport route through the rock which also leads the species into the fracture with a known water concentration (c_∞=0) was recently studied

(Lee et al., 1989). Analytical expressions were devised which allows for the calculation of the transport into a small slit from the clay (Lee et al, 1989). The numerical model has been extended to also handle the transport to the flowing water in the fracture with a concentration profile which was built up by instationary diffusion into the slowly flowing water in the fracture (App II). In this numerical model also presence of clay in the mouth of the fracture was included. This model, although more sophisticated than the previous cannot handle the buildup of the concentration profile in the water in the fracture correctly. To do this it would be necessary to use a fully 3-dimensional solution describing the hole with its clay plug, the rock with the fracture and the flowing water in the fracture. This has recently been done (see App II), showing that for the combination of parameter values that can be expected, the error is small. The reason is that the concentration profile in the water in the rock extends for many tens of centimeters whereas only the first few centimeters of the rock nearest the edge of the fracture will transport any appreciable amounts of dissolved species.

As an extension to the extended model (a hole in the canister wall) an additional transport path is added, leading from the damaged canister through the backfill to the disturbed zone surrounding the tunnel above the repository holes.

2.1.4 Transport in the water in the fracture

Water flows in the fracture and it will pick up more and more dissolved species as it flows past the clay in the hole. For an idealized fracture consisting of a parallel walled slit with potential flowrate a solution for the diffusion equation was used (Neretnieks 1980). The same solution has subsequently been derived also stating error bounds by Pigford et al. (1990). Andersson et al (1981) incorporated this notion in a 3-dimensional model calculation where the diffusion through the backfill to the fracture and the onward diffusion into the passing water was calculated.

3 RESISTANCE MODEL

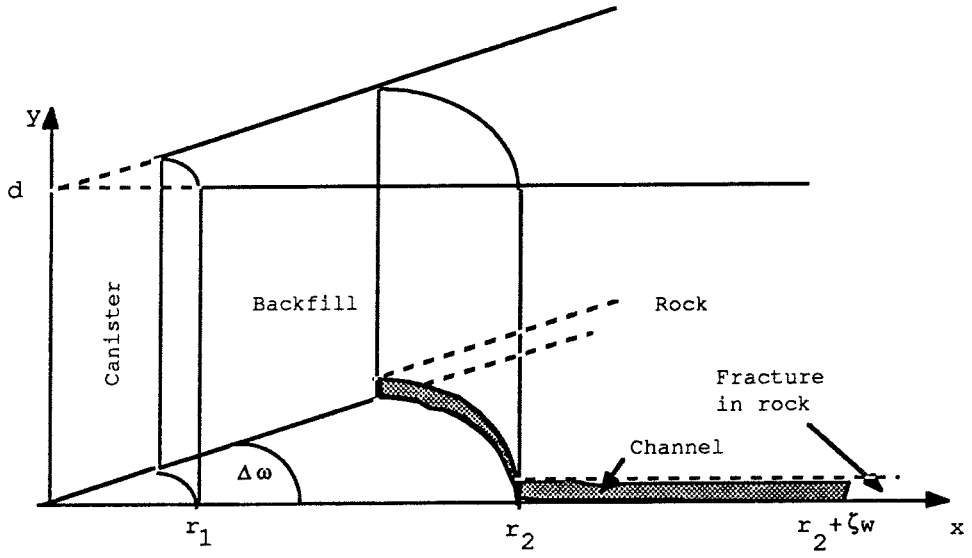

Figure 2. A sector of the backfill with the canister and the rock with the fracture.

The transport of radionuclides from a damaged canister can be subdivided into two main transfer processes:

1) diffusion perpendicular to the flow in the channel and
2) advective transport of dissolved species along the channel

each of these main processes will in its turn consist of a number of subprocesses.

The subprocesses that will be considered for the diffusion perpendicular to the flow are

* diffusion through the backfill to the fracture mouth
* diffusion through a plug of backfill, penetrated into the fracture by σ m.
* transfer into the flowing water in the channel, via the fracture mouth
* diffusion via the rock to the fracture ceiling/floor
* transfer from the fracture ceiling/floor into the flowing water
* diffusion from the fracture ceiling/floor into a penetrated plug of backfill material

For each of the subprocesses the contribution to the total flowrate of radionuclides into the channel can be calculated as $N_i = k_i A_i \Delta c_i$ where k_i is the mass transfer coefficient for subprocess i.

The total flowrate of dissolved species into the flowing water in the fracture will be calculated by coupling the resistances to the mass transfer by the different subprocesses ($R_i = 1/k_i A_i$) to a total mass transfer resistance ($R_t = 1/k_t A_t$) from which the flowrate of nuclides can be calculated as $N_t = k_t A_t \Delta c_t$.

For a simple geometry this resistance can be derived from Fick's law

$$N = - D \cdot A \cdot \frac{\partial C}{\partial x} \approx \frac{D \cdot A}{x} \cdot \Delta C \qquad (1)$$

and

$$\frac{1}{R} = \frac{D \cdot A}{x} \quad \text{or} \quad R = \frac{x}{D \cdot A} \qquad (2)$$

where x is the diffusion length and A the diffusion cross section.

For the modelling of the diffusion process a sector of the canister together with connecting back-fill, rock and fracture with the boundaries $0<y<d$, $0<x<r_2+\zeta w$ and $\omega<\theta<\omega+\Delta\omega$ (see figure 2) is regarded. For not too small r_1, compared with r_2 the geometry of the sector can be transformed to a parallel-epiped, whereby rectangular symmetry is achieved.

3.1 Resistance model when canister wall is completely corroded.

The transport of nuclides from a damaged canister through the nearfield can be described by a network of transport resistances, coupled together in the same way as an electrical circuit network. The starting potential for this network, c_0 is the nuclide concentration on the outside of the corroded canister.

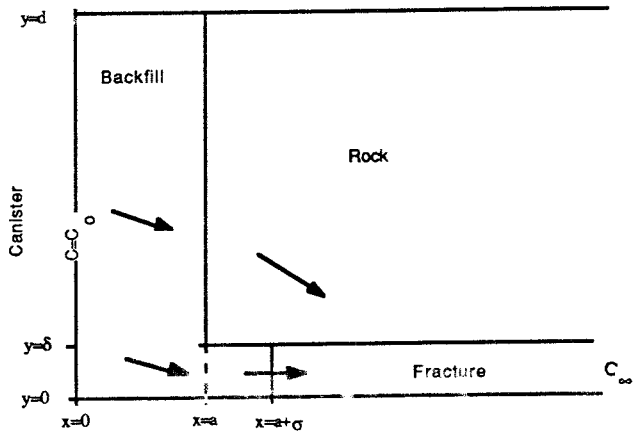

Figure 3. Transport routes from the canister to the fracture.

The simplest case would be that the transport though the rock matrix is coupled in parallel with the transport through the film resistance in the flowing water in the fracture. The resistance network would then be

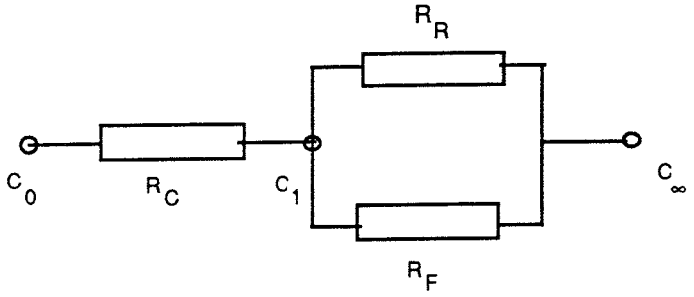

In this case the nuclide concentration will be the same in the fracture mouth and along the backfill-rock interface. Furthermore is the film resistance over the rock-fracture interface neglected. The total resistance for the system then becomes

$$R_O = R_C + \frac{R_R \cdot R_F}{R_R + R_F}$$

If we instead consider the transport routes through the backfill-fracture mouth and backfill-rock-fracture as two separated independent transports we can describe the system as

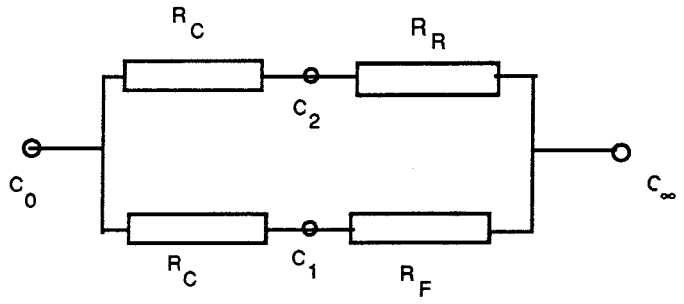

This model will give a step change in concentration as we move from the fracture mouth to the rock face.. The weakness of both these models is that a mean value of the rock resistance is very difficult to evaluate properly.

As the rock resistance at the very edge will be very small, compared to that of the main part of the rock matrix as well as the film resistance, the model will produce a very large nuclide transport at the very edge.

One way of solving this problem is to consider the area near the edge separately, treating the edge as part of the fracture opening. Conceptually this is maybe a little problematic, since it is not possible to define the extension of this edge area in terms of an absolute distance or as a fraction of the width of the fracture opening.

If, however we assume that the backfill clay will penetrate into the fracture opening, even for a very short distance, even as short as one or a part of a fracture width a model solution becomes quite obvious.

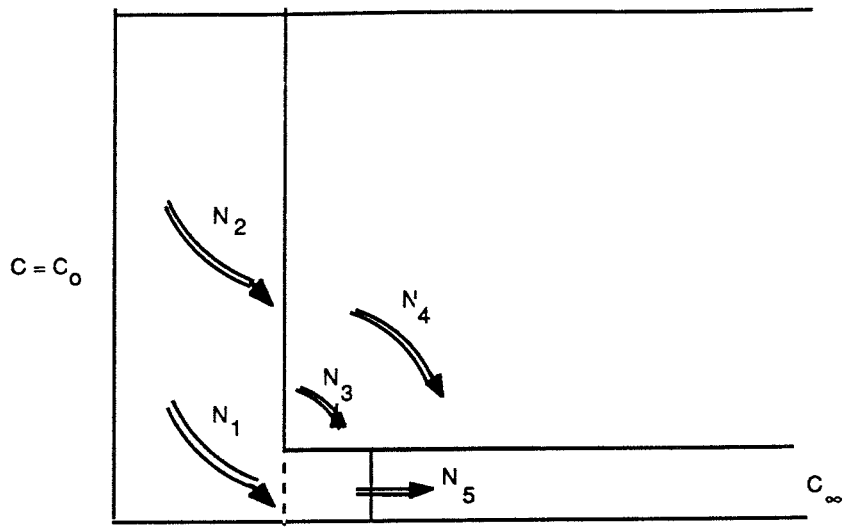

Figure 4. Diffusion routes with a clay plug penetrating into the fracture.

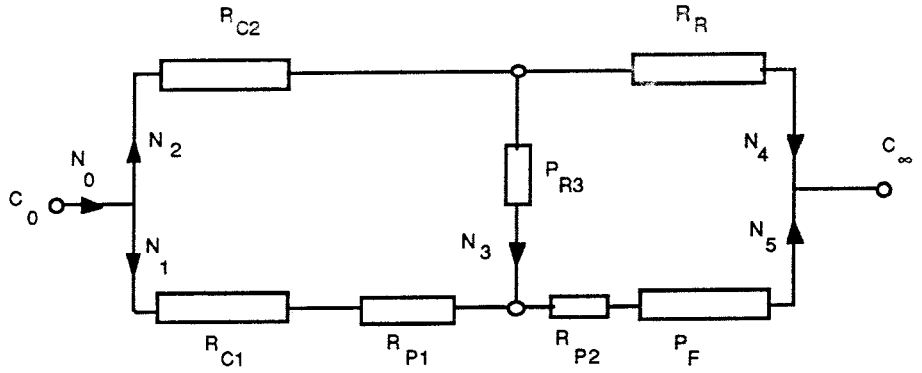

R_{C1}, R_{C2}	Resistance in the backfill clay	
R_{P1}, R_{P2}	-"-	in the clay plug
R_{R3}	-"-	in the rock edge
R_R	-"-	in the rock matrix
R_F	Equivalent film resistance	in the fracture water

Figure 5. Resistance model with a clay plug penetrating into the fracture mouth.

As the nuclides migrate into the flowing water in the fracture a concentration profile develops in the water close to the fracture mouth. This profile is a result of a mass transfer resistance in the water as described by Neretnieks, (1986). By placing the film resistance after the connections between N_4, N_6 to N_5 we introduce the effect that the diffusion streams through the rock and the edge will enter the fracture at a point quite close to the interface between the clay

plug and the fracture water, consequently it will diffuse against a concentration quite close to that of the mentioned interface.

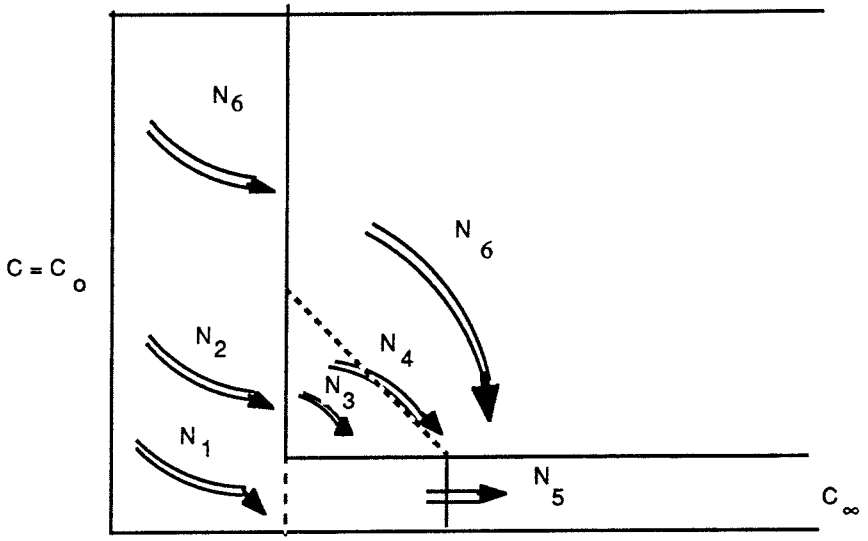

Figure 6. Diffusion model with the rock matrix sectioned in one edge and one rock cell.

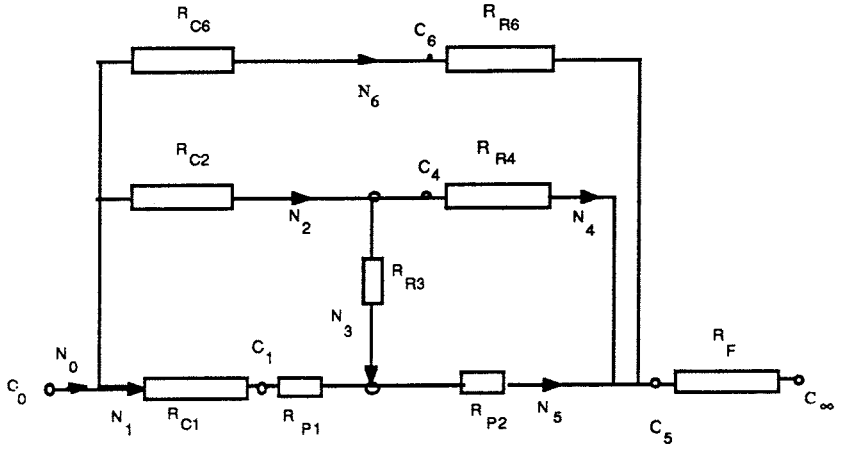

Figure 7. Resistance model corresponding to the model in figure 6.

The solution is carried out stepwise. As a first step we resolve the inner network, equivalent to that of Figure 5. For solution purposes the network is pictured as

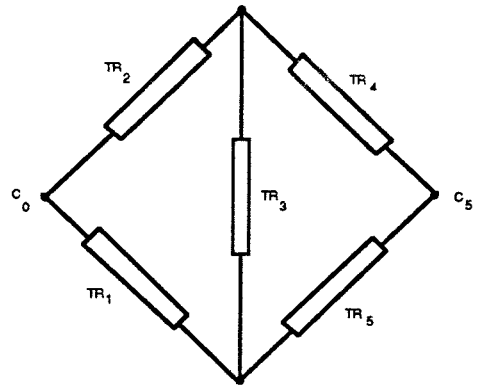

Where $TR_1 = R_{C1} + R_{P1}$
$TR_2 = R_{C2}$
$TR_3 = R_{R3}$ (3a -3e)
$TR_4 = R_R$
$TR_5 = R_{P2}$

The resulting overall resistance is calculated the same way as electrical resistance circuits are evaluated. According to the rule of star-polygon transformation any star of resistances can be replaced by a polygon with the same nodes, such that all potentials and streams outside the nodes remain unchanged. The rule is of course reversible.

For the simple case of a triangle, as in our model we get

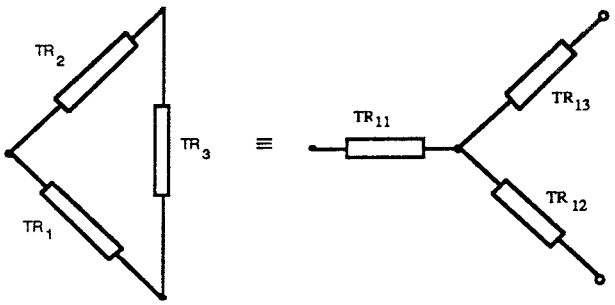

$$TR_{11} = \frac{TR_1 \cdot TR_2}{TR_1+TR_2+TR_3} \quad ...(4a)$$

$$TR_{12} = \frac{TR_1 \cdot TR_3}{TR_1+TR_2+TR_3} \quad ...(4b)$$

$$TR_{13} = \frac{TR_2 \cdot TR_3}{TR_1+TR_2+TR_3} \quad ...(4c)$$

and for the coupled triangles

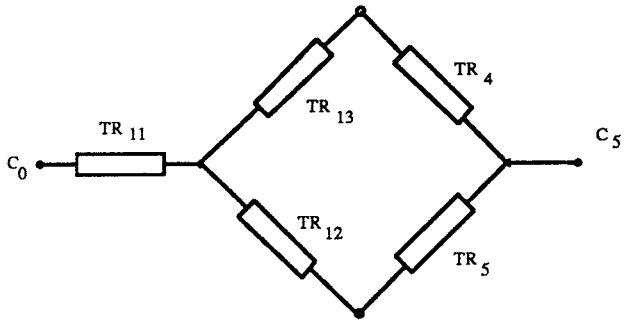

with the resulting resistance

$$R_{\square} = TR_{11} + \frac{(TR_4+TR_{13})(TR_5+TR_{12})}{TR_4+TR_5+TR_{12}+TR_{13}} \quad (5)$$

With the rock segmented into two parts, the "edge" and one "rock cell" the model described here is supplemented with a pair of resistances R_{C6} and R_{R6},

coupled in parallel across the network, as in figure 7. The resulting resistance for this part of the network becomes

$$R_0'' = \frac{1}{\frac{1}{R_0'} + \frac{1}{R_{C6}+R_{R6}}} \tag{6}$$

Finally we add the equivalent film resistance, R_F coupled in series with the rest of the network. Consequently the resulting diffusion resistance for the whole network becomes

$$R_{Res} = R_0'' + R_F \tag{7}$$

3.2 Diffusion through the backfill to the rock interface - canister wall completely corroded

The result of an evaluation of the mass transfer resistance is greatly dependent on a correct estimation of the parameters for diffusion length and cross sectional area. Especially critical are the values to be used for estimation of the resistances in the backfill for diffusion through the clay into the fracture mouth, since the height of the segment varies from d to $\frac{\delta}{2}$ from the canister surface to the fracture opening and the diffusion lengths from a to $\sqrt{a^2+d^2}$.

With the above mentioned assumptions the transport equation can be expressed in Cartesian coordinates

$$\frac{\partial^2 c}{\partial x^2} + \frac{\partial^2 c}{\partial y^2} = 0 \tag{8}$$

with the following boundary conditions

$$\frac{\partial c}{\partial y} = 0 \qquad \text{for } 0<x<a,\ y=0 \tag{9}$$

$$\frac{\partial c}{\partial y} = 0 \qquad \text{for } 0<x<a,\ y=d \tag{10}$$

$$c=c_0 \qquad x=0\ (r=r_1) \quad 0<y<d \tag{11}$$

and

$$\frac{\partial c}{\partial x} = f(y) \qquad x=a\ (r=r_2)\ ,\ 0<y<d \qquad (12)$$

We assume that there are two competing transport routes through the backfill into the fracture, one (1) leading through the backfill to the fracture mouth, the other (2) via the interface between backfill and rock through the rock matrix to the fracture ceiling/floor.

Furthermore a calculation made with the assumption of c=0 in the fracture (Lee et al, 1989) shows that the concentration along the backfill/rock interface very close to the fracture edge assumes a constant value. Since the actual concentration in the fracture, at least close to the fracture mouth will have finite values the concentration profile along the rock surface will reach a constant value even closer than indicated by Lee.

Let us assume that the contribution to the total flowrate via route 1 is $N'=\varphi \cdot N$ and via route 2 $N''=(1-\varphi)\cdot N$, so

$$f'(y) = \frac{\varphi \cdot N}{A_{fiss} \cdot D_1} \qquad 0<y<\frac{\delta}{2}$$

and

$$f''(y) = \frac{(1-\varphi) \cdot N}{A_{rock} \cdot D_1} \qquad \frac{\delta}{2}<y<d$$

This indicates that the flux is considered as constant over the fracture mouth, $0<y<\frac{\delta}{2}$. At $y=\frac{\delta}{2}$ there is a step change in flux to another constant value along the backfill/rock interface.

By treating the two transport routes separately, calculating the diffusion rates for each route, assuming the flux across the other barrier is zero we can determine the respective contribution to the total transport resistance through the backfill from the two routes and also find an representation of the concentration profile at the backfill/rock matrix interface.

For transport only through the fracture mouth the boundary condition at $x=r_2$ is

$$\frac{\partial c}{\partial x} = f'(y) \text{ where } f'(y)=\text{const at } 0<y<\frac{\delta}{2} \text{ and } =0 \text{ at } \frac{\delta}{2}<y<d$$

For this case the solution of eq 1 (Lee et al 1989) gives

$$\frac{c}{c_0} = 1 - \frac{N}{A\cdot D\cdot c_0}\left(\frac{\delta}{2\cdot d}a + \sum_{n=1}^{\infty} \frac{2d}{(n\pi)^2}\cos\left(\frac{n\pi}{d}y\right)\sin\left(\frac{n\pi}{d}\frac{\delta}{2}\right)\frac{\sinh\left(\frac{n\pi}{d}x\right)}{\cosh\left(\frac{n\pi}{d}a\right)}\right) \qquad (13)$$

or rearranged to give the equivalent nuclide flowrate

$$\frac{N}{c_0-c} = \frac{A\cdot D}{\left(\frac{\delta}{2\cdot d}a + \sum_{n=1}^{\infty} \frac{2d}{(n\pi)^2}\cos\left(\frac{n\pi}{d}y\right)\sin\left(\frac{n\pi}{d}\frac{\delta}{2}\right)\frac{\sinh\left(\frac{n\pi}{d}x\right)}{\cosh\left(\frac{n\pi}{d}a\right)}\right)} \qquad (13a)$$

From this expression we get the average value of $\frac{x}{A}$ in (eq. 1) for the calculated transport route as

$$\frac{(c_0-c)\cdot D}{N} = \left(\frac{\overline{x}}{A}\right) = \frac{\frac{\delta}{2\cdot d}a + \sum_{n=1}^{\infty} \frac{2d}{(n\pi)^2}\cos\left(\frac{n\pi}{d}y\right)\sin\left(\frac{n\pi}{d}\frac{\delta}{2}\right)\frac{\sinh\left(\frac{n\pi}{d}x\right)}{\cosh\left(\frac{n\pi}{d}a\right)}}{A_{fract}} \qquad (14)$$

This equation has been developed for a case where the diffusion leads to an opening situated between y=0 and y=δ/2. In order to accommodate the calculations of the diffusion routes to the rock surface a more generalized form of the solution is needed.

The general solution to the diffusion equation in the two-dimensional region (0<y<d and 0<x<a) (Özisik and Mikhailov, 1984) with the boundary conditions

$$c|_{x=0} = \text{const} = c_0 \qquad (15)$$

$$\frac{\partial c}{\partial y}\Big|_{y=0} = \frac{\partial c}{\partial y}\Big|_{y=d} = 0 \tag{16}$$

$$\frac{\partial c}{\partial x}\Big|_{x=a} = Q_0 \cdot f(y) \quad \text{where} \tag{17}$$

$$f(y) = \left\{ \begin{array}{ll} 1 & \text{for } \beta \le y \le \beta+\upsilon \\ 0 & \text{for all other values} \end{array} \right\} \qquad (0 \le \beta \le d) \tag{18}$$

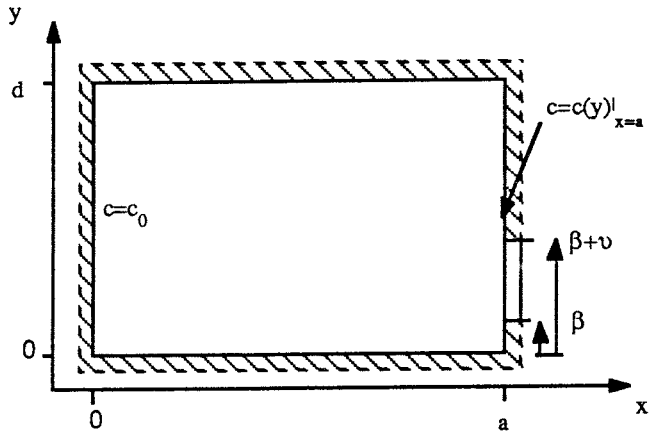

Figure 8. Schematic view of the region near the canister for diffusion to an arbitrary section at x=a.

$$\overline{\left(\frac{X}{A}\right)} \cdot A_{fract}\Big|_{x=a} = Q_0 \cdot \frac{a}{d} \cdot \int_0^d f(y)dy + 2 \cdot \sum_{n=1}^{\infty} \cos\left(\frac{\pi n y}{d}\right) \cdot Q_0 \cdot \int_0^d f(y) \cdot \cos\left(\frac{\pi n y}{d}\right) dy \cdot \frac{1}{\pi \cdot n} \tanh\left(\frac{\pi n a}{d}\right) \tag{19}$$

The term $\overline{\left(\frac{X}{A}\right)} \cdot A_{fract}$ is equivalent to the summation function F(x,y) in (Lee et al, 1989) and can be regarded as an equivalent diffusion length of a clay plug with the area A_{fract} from which the transport resistance for the diffusion through the backfill to the fracture mouth can be calculated.

If Q_0=1 the expression is evaluated for the mid point of the section ($y=\beta+\frac{\upsilon}{2}$) to

$$F(a, (\beta+\tfrac{\upsilon}{2})) = \frac{a}{d}\int_0^d f(y)dy + 2\cdot\sum_{n=1}^{\infty} \cos\left(\frac{\pi n y}{d}\right)\cdot\int_\beta^{\beta+\upsilon} f(y)\cdot\cos\left(\frac{\pi n y}{d}\right) dy\cdot\frac{1}{\pi\cdot n}\tanh\left(\frac{\pi n a}{d}\right) \quad (20)$$

$$F(a, (\beta+\tfrac{\upsilon}{2})) = \frac{a\cdot\upsilon}{d} + \sum_{n=1}^{\infty} \frac{2}{\pi\cdot n}\cos\left(\frac{\pi n(\beta+\frac{\upsilon}{2})}{d}\right)\cdot\left|\frac{d}{\pi\cdot n}\sin\left(\frac{\pi n y}{d}\right)\right|_\beta^{\beta+\upsilon}\cdot\tanh\left(\frac{\pi n a}{d}\right) \quad (21)$$

$$F(a, (\beta+\tfrac{\upsilon}{2})) = \frac{a\cdot\upsilon}{d} + \sum_{n=1}^{\infty} \frac{2d}{(\pi\cdot n)^2}\cos\frac{\pi n(\beta+\frac{\upsilon}{2})}{d})\cdot(\sin\left(\frac{\pi n(\beta+\upsilon)}{d}\right) - \sin\left(\frac{\pi n\beta}{d}\right))\cdot\tanh\left(\frac{\pi n a}{d}\right) \quad (22)$$

$$F(a, (\beta+\tfrac{\upsilon}{2})) = \frac{a\cdot\upsilon}{d} + \sum_{n=1}^{\infty} \frac{4d}{(\pi\cdot n)^2}\cos^2\left(\frac{\pi n(\beta+\frac{\upsilon}{2})}{d}\right)\cdot\sin\left(\frac{\pi n\frac{\upsilon}{2})}{d}\right)\cdot\tanh\left(\frac{\pi n a}{d}\right) \quad (23)$$

For ratios of $\frac{\upsilon}{d}<<1$ simplifications will give large errors since the amplitude of the oscillating summation term will be large.

3.3 Mass transfer resistances

The parameters for the diffusion in the rock matrix are easier to estimate.

The "edge" is arbitrarily defined as having the same height as length = the penetration length of the clay plug = σ.

The diffusion route through the rock via the clay plug will enter the plug at a distance $\frac{\sigma}{2}$ from the fracture mouth. The diffusion routes through the edge and the rock matrix to the fracture roof will enter the fracture very close to the leading front of the plug, i.e. at a distance of σ from the fracture mouth.

The cross sectional areas of the rock segments are taken as the segment area on the interface between rock and backfill.

1. Resistance in the backfill clay leading to the fracture mouth, R_{C1}

$$R_{C1} = \frac{F(x,y)}{A_{fract} \cdot D_C} \tag{24}$$

where F(x,y) is the value of the equation (16) at a position x=a and in a fracture with a width of $\upsilon=d/2$ and with $\beta=0$.

2. Resistance in the backfill clay leading to the rock edge (R_{C2}).

$$R_{C2} = \frac{F(x,y)}{A_{edge} \cdot D_C} \tag{25}$$

where F(x,y) is the value of the equation (16) at a position x=a for an edge with a width of $\upsilon=\sigma$ and with $\beta=\delta/2$. Furthermore we assume that $\delta/2 \leq \sigma \leq d-\delta/2$.

3. Resistance in the backfill clay leading to the rock matrix (R_{C6})

$$R_{C6} = \frac{F(x,y)}{A_{rock} \cdot D_C} \tag{26}$$

where F(x,y) is the value of the equation (23) at a position x=a for a rock cell with a height of $\upsilon=d-\delta/2-\sigma$ and with $\beta = \delta/2+\sigma$.

4. Resistance in the rock edge for the flow going via the clay plug (R_{R3}).

$$R_{R3} = \frac{1}{\pi \cdot r_2 \cdot D_R \cdot \ln(2+\sqrt{5})} \tag{27}$$

5. Resistance in the rock edge for the flow via the fracture roof (R_{R4}).

$$R_{R4} = \frac{1}{\pi \cdot r_2 \cdot D_R \cdot \ln(1+\sqrt{2})} \tag{28}$$

6. Resistance in the rock matrix (R_{R6})

$$R_{R6} = \frac{1 \cdot}{\pi \cdot r_2 \cdot D_R \cdot \ln\left(\frac{(d-\frac{\delta}{2})+\sqrt{(d-\frac{\delta}{2})^2+\sigma^2}}{\sigma \cdot (1+\sqrt{2})}\right)} \tag{29}$$

As for R_{C6} this expression can be used as long the plug is shorter than the distance to the system boundary in the y-direction, that is for all $\sigma < (d-\delta/2)$. For $\sigma \geq (d-\delta/2)$ R_{R6} is let to be ∞.

7. Resistance in the clay plug, (R_{P1}, R_{P2})

$$R_{P1} = \frac{\ln(\frac{r_2+\frac{\sigma}{2}}{r_2})}{\pi \cdot \delta \cdot D_P} \quad \text{and} \quad R_{P2} = \frac{\ln(\frac{r_2+\sigma}{r_2+\frac{\sigma}{2}})}{\pi \cdot \delta \cdot D_P} \tag{30}$$

8. Film resistance, (R_F)

$$R_F = \sqrt{\frac{\Omega}{4 \cdot \pi \cdot D_W \cdot u_f \cdot (r_2+\sigma) \cdot \delta^2}} \tag{31}$$

Table 1. Data used in calculations

Backfill diffusivity	$D_C = 4 \cdot 10^{-11}$	[m^2/s]
Clay plug diffusivity	$D_P = 4 \cdot 10^{-10}$	[-"-]
Rock diffusivity	$D_R = 7{,}4 \cdot 10^{-13}$	[-"-]
Water diffusivity	$D_W = 3.9 \cdot 10^{-9}$	[-"-]
Canister radius	$r_1 = 0.375$	[m]
Radius of bore hole	$r_2 = 0.75$	[m]
Angle at which the film resistance is calculated	$\Omega = \pi/4$	[rad]

The resistance models cannot satisfactorily handle penetration lengths (σ) = 0. If, however, the lower boundary for σ is set at any value > 0 the model can be applied.

When σ becomes larger than d (half the fracture spacing) the calculations of the backfill resistances for the diffusion routes leading to the rock matrix yield erroneous results. Therefore the length of the rock/backfill interface must be limited to (d-δ/2) even if the plug penetration is greater than that.

The equation for the resistance R_{R6} also has a validity limit at σ=(d-δ/2). At σ=(d-δ/2) it will yield division by zero and for σ>(d-δ/2) give negative values of R_{R6}. The limit value for R_{R6} as $\sigma \rightarrow$(d-δ/2) is ∞.

The resistances calculated for the transport routes through the backfill clay become conservative approximations, since the resistances are superimposed, i.e in any point in the backfill the model assumes that diffusion takes place towards each of the sectors at the interface backfill/fracture mouth - rock surface instead of along the route with the steepest concentration gradient.

3.4 Diffusion in the backfill with a hole in the canister wall

For the case where the canister is subject to a local corrosion attack, we can assume that the penetration of the canister wall will be in the form of a cylindrical hole of limited size, e.g. with a diameter of λ m.

Since the diffusion source on the canister wall has an entirely different geometry than the fracture and the rock wall have as diffusion recipients an analytical solution of the transport of nuclides through the backfill will require a 3-dimensional solution of the diffusion equation (eq. 8). For modelling purposes this is not practical, therefore a simplified approach is proposed, connecting the effect of the reduced size of the diffusion source to the resistance model based on a completely corroded canister wall, developed in chapter 3.1.

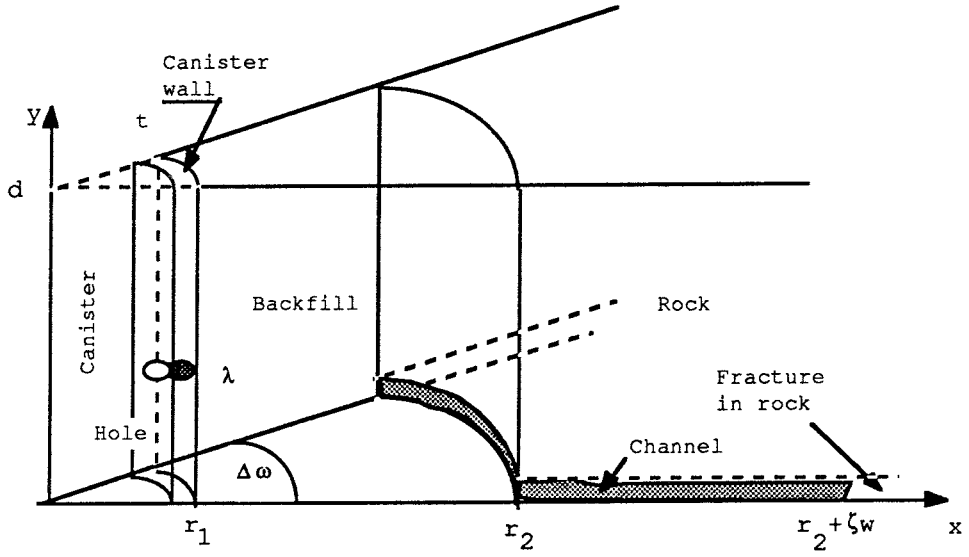

Figure 9. Sector of a canister with a hole in the wall

In a three-dimensional solution of the case assuming that the entire canister wall had been corroded it has been shown (App II) that the concentration profile in the bentonite filling very close to the fracture mouth reaches a value quite close to that of the concentration at the canister (c_0). Here the resistance to the mass transfer is described by

$$R_{C1} = \frac{F(x,y)}{A_{fract} \cdot D_C} \tag{24}$$

This indicates that we in this two-dimensional model conceptually can visualize the resistance in the clay backfill to the flow into the fracture mouth as concentrated to a bentonite plug with a length of $F(a,\frac{\delta}{2})$ and a cross sectional area of A_{fract}. In the same way the resistances to flow through the backfill to the rock wall (edge and rock cell) can be replaced by bentonite plugs with cross sectional areas equal to the edge and rock cell respectively and with lengths equal to the value of $F(a, (\beta+\frac{\upsilon}{2}))$ from (eq. 23). Outside these plugs the rest of the bentonite backfill has the same concentration as at the canister wall, c_o.

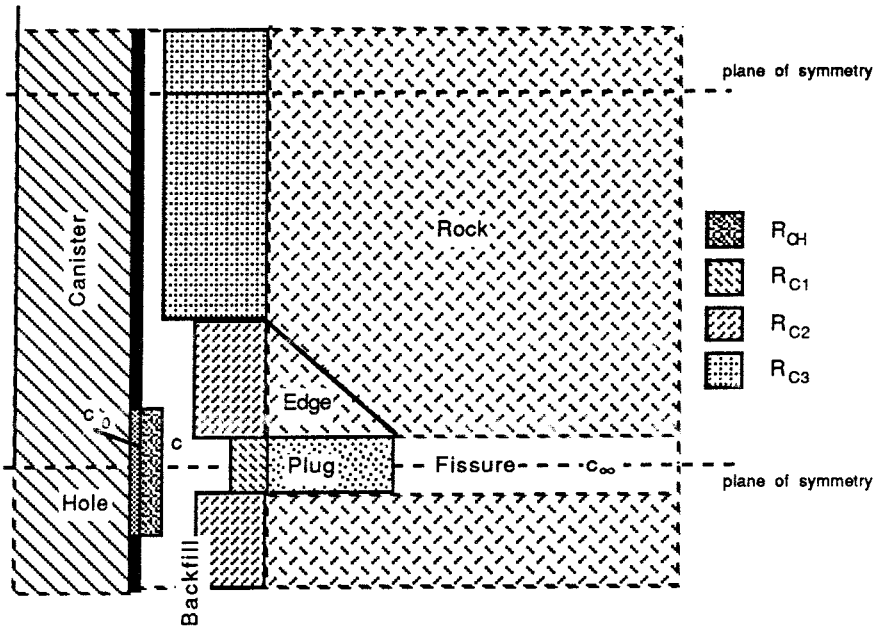

Figure 10. Equivalent mass transfer resistances

If we now reintroduce the canister wall with a cylindrical hole, with a diameter of λ m, filled with corrosion products the release of nuclides from the canister is reduced considerably since the diffusion rate is directly proportional to the mass transfer area.

This reduction of nuclide release can be considered as a result of an additional mass transfer resistance, in the opening of the hole in the canister wall.

With this representation of the mass transfer resistances in the system we can see how the concentration profile will develop. Starting inside the canister wall, where the initial concentration is c_i, the concentration will fall due to the transport resistance, R_{Corr}, exerted by the corrosion products in the hole and

subsequently by the equivalent entry resistance R_{CH} to a concentration plateau, c, represented by the white area in the backfill in figure 10. This area of constant concentration will extend in a continuous band, however thin, throughout the backfill.

Downstream this concentration plateau the resistance model remains exactly the same as in the earlier model (figure 7). Consequently in order to describe the nuclide transport for this case the resistance network developed for the completely corroded canister only needs to be complemented with the resistance $R_{Hole} = R_{Corr} + R_{CH}$ coupled in series in front of the former network.

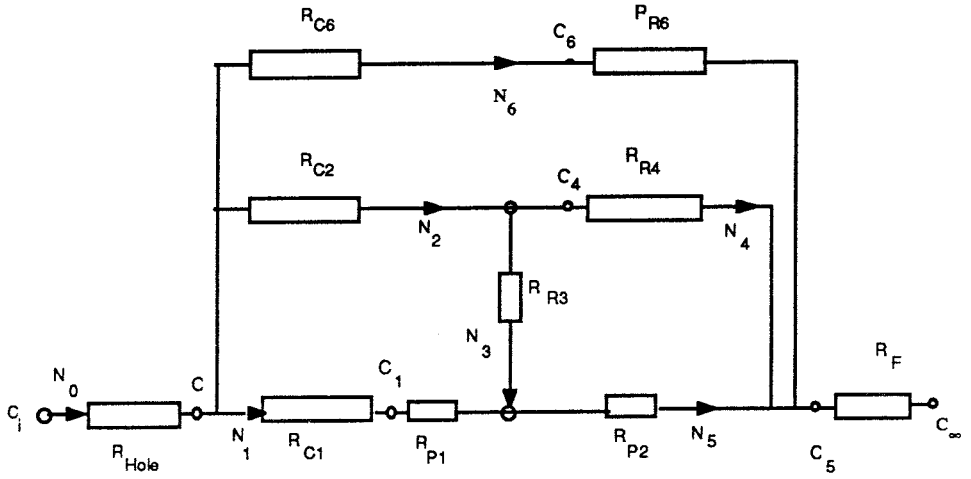

Figure 11. Resistance network with a hole in the canister wall

The value of this entry resistance can easily be calculated, if we can assume that the corrosion products in the hole will protrude into the backfill clay to form a semi-sphere. With the further assumption that the concentration on the surface of this semi-sphere is uniform and = c the transport of nuclides into the backfill clay will proceed radially from this area. If the hole is small compared to the thickness of the backfill assumptions will introduce relatively small errors.

For the mass transfer from a sphere into a surrounding medium the transfer rate will be

$$N = - D \cdot A \cdot \frac{dC}{dr} = - 4 \cdot \pi \cdot r^2 \cdot D \cdot \frac{dC}{dr} \qquad (32)$$

Integrating between the limits r_{sphere} and r

$$N \cdot \int_{r_{sphere}}^{r} \frac{dr}{r^2} = 4 \cdot \pi \cdot D \cdot \Delta C \tag{33}$$

$$N = \frac{4 \cdot \pi \cdot D \cdot \Delta C}{\frac{1}{r_{sphere}} - \frac{1}{r_2}} \tag{34}$$

If the concentration difference is spread over a large distance, so that $r >> r_{sphere}$ we get

$$\frac{r_{sphere} \cdot N}{4 \cdot \pi \cdot r_{sphere}^2 \cdot \Delta C \cdot D} = 1 \tag{35}$$

Defining the mass transfer coefficient $k_i = \frac{N}{A \cdot \Delta C} = \frac{N}{4 \cdot \pi \cdot r_{sphere}^2 \cdot \Delta C}$ the expression can be transformed to

$$\frac{k_i \cdot r_{sphere}}{D} = 1 \qquad \text{or} \qquad \frac{k_i \cdot d_{sphere}}{D} = 2 \tag{36}$$

As discussed on p. 7 in this report the mass transfer resistance is related to the mass transfer coefficient as $R_i = \frac{1}{k_i \cdot A_i}$ we get for this case $k_{CH} = \frac{1}{R_{CH} \cdot A_{1/2sphere}}$ and $d_{sphere} = d_{hole} = \lambda$.

From equation (36) we get

$$R_{CH} = \frac{1}{\pi \cdot \lambda \cdot D_C} \tag{37}$$

By analogy with the other backfill resistances R_{CH} can be regarded as an equivalent clay plug with the same area as the hole, $(\frac{\pi \cdot \lambda^2}{4})$, and a length that in this case is equal to one quarter of the hole diameter, $(\frac{\lambda}{4})$.

The mass transfer resistance in the hole in the canister wall depends on how and when the damage occurs. If there is a construction error causing the hole it is reasonable that the mass transfer resistance is calculated as a cylindrical plug of stagnant water with a diameter of λ m and a length of the canister wall thickness t = 0.06 m. If on the other hand the damage is caused by pit

corrosion the mass transfer resistance is due to a plug of corrosion products. In the latter case the resistance is calculated as

$$R_{Corr}=\frac{4\cdot t}{\pi\cdot\lambda^2\cdot D_{Corr}} \tag{38}$$

D_{Corr} is the effective diffusivity in the plug of corrosion products. It can be estimated from the diffusivity in pure water corrected with the relative volume available to diffusion, equivalent to the porosity of the plug, ε, and the diffusion length, which is related to the tortuosity or the windling factor of the plug, τ.

$$D_{Corr} = D_W\cdot fkn(\varepsilon,\tau) \tag{39}$$

Since the precipitation of corrosion products in the hole proceeds at a very low rate and under high pressure, it is reasonable to assume that the plug of corrosion products will consist of a dense lattice of relatively large crystals. Thus the porosity will be low, probably in the same order of magnitude as the compacted bentonite, though with a larger tortuosity as a result of the larger particles. The effective diffusivity will therefore be larger than that of the backfill, but considerably less than that of pure water. A reasonable estimate of the effective diffusivity of the plug of corrosion products is $4\cdot10^{-10}$ m^2/s.

The equivalent resistance of the hole, $R_{Hole} = R_{Corr} + R_{CH}$ thus becomes

$$R_{Hole}=\frac{1}{\pi\cdot\lambda}\cdot\left(\frac{4\cdot t}{\lambda\cdot D_{Corr}}+\frac{1}{D_C}\right) \tag{40a}$$

For the case of a hole caused in the fabrication process the equivalent resistance becomes

$$R_{Hole}=\frac{1}{\pi\cdot\lambda}\cdot\left(\frac{4\cdot t}{\lambda\cdot D_W}+\frac{1}{D_C}\right) \tag{40b}$$

3.5 Diffusion in the backfill with a slit in the canister wall

The third alternative type of damage to the canister is that caused by a shearing of the canister resulting in a fracture extending around the entire canister perimeter. Also this type of damage will result in a considerably lower release rate of nuclides compared to the case with completely corroded canister wall. To estimate the effect on the release of nuclides by the fracture we can use the same line of reasoning as for the circular hole in the canister, i.e. we can represent the resistance to the mass transfer by a plug of backfill with the same area as the fracture and with a length corresponding to the value of the factor F(x,y) in eq. 24 evaluated as F(a,γ) where γ is the aperture of the canister fracture.

The resistance of this plug is thus

$$R_{SC}=\frac{F(x,\gamma)}{2\cdot\pi\cdot r_1\cdot\gamma\cdot D_C} \tag{41}$$

The value of the factor F(a,γ) is for $0.001 < \frac{\gamma}{a} < 0.1$ between 2 and 6 times the aperture, i.e. F(a,γ) = 2γ - 6γ. the value decreasing as the aperture increases. For this case let us assume a value of 4γ. This will result in an equivalent slit exit resistance of

$$R_{SC}=\frac{4\cdot\gamma}{2\cdot\pi\cdot r_1\cdot\gamma\cdot D_C}=\frac{2}{\pi\cdot r_1\cdot D_C} \tag{42}$$

i.e. the resistance is independent of the fracture aperture.

Since the damage to the canister can occur at any time the diffusion resistance in the fracture itself is calculated as if the space in the fracture is filled with pure liquid, i.e. no corrosion products inhibit the diffusion from the inside of the canister through the fracture until the nuclides reach the backfill. The resistance in the fracture is therefore calculated with an effective diffusivity equal to that of water $D_{Frac} = D_W = 3.9\cdot10^{-9}$ m^2/s.

If the thickness of the canister wall is small compared to the canister radius the resistance in the fracture thus becomes

$$R_{Frac}=\frac{t}{2\cdot\pi\cdot r_1\cdot\gamma\cdot D_W} \tag{43}$$

and the equivalent resistance of the whole rupture system $R_{Rupt} = R_{SC} + R_{Frac}$.

$$R_{Rupt} = \frac{t}{2 \cdot \pi \cdot r_1 \cdot \gamma \cdot D_W} + \frac{2}{\pi \cdot r_1 \cdot D_C} = \frac{1}{2 \cdot \pi \cdot r_1} \left(\frac{t}{\gamma \cdot D_W} + \frac{4}{D_C} \right) \quad (44)$$

This means that the ratio $\frac{t}{\gamma}$ will influence the mass transfer rate in the rupture if it is in the same order of magnitude or larger than $\frac{D_W}{D_C}$ or 100. With a canister wall thickness of 60 mm the mass transfer resistance in the canister fracture will have a significant influence if the aperture is in the order of 1 mm or less.

3.6 Diffusion through the bore hole backfill to the disturbed zone

In addition to the transport paths described above, an other outflux route of potential importance can be identified. This is the transport of nuclides through the backfill in a vertical direction towards the transport tunnel above the repository hole and into the water flowing in the so called "disturbed zone". This disturbed zone is a highly conductive fracture zone that is developed around the transport tunnel as a result of the drilling of the tunnel (Figure 12).

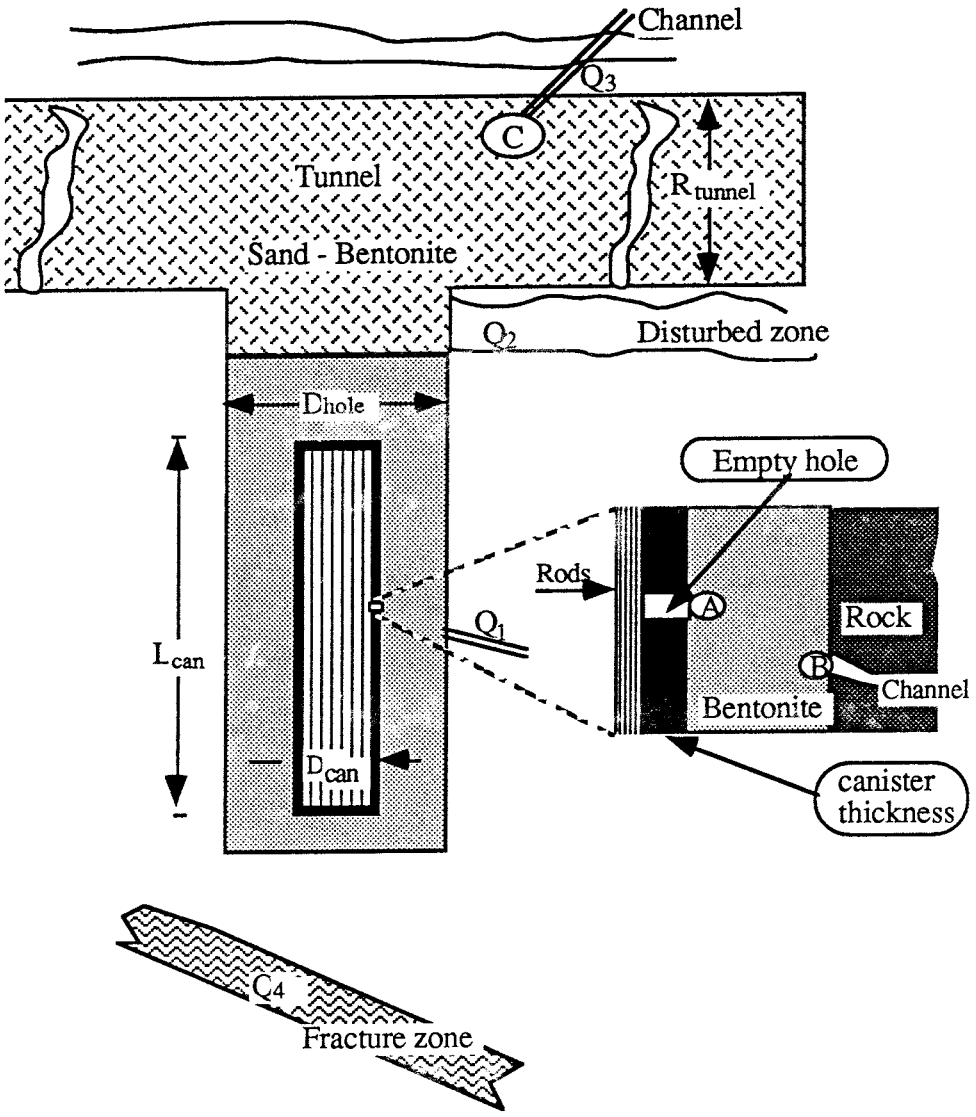

Figure 12. Repository for used nuclear fuel, showing anticipated fracture zones in the rock matrix.

In order to include this case into the basic resistance network model we assume that the diffusion source is a plane across the entire repository hole at the level of the top of the canister. We assume further that the concentration profile in the system has developed in the way described in chapter 3.3, i.e. the concentration along the plane over the entire cross section is uniform as equal to that on the outside of the canister surface, including a potential concentration difference caused by an entry resistance as in the cases with limited canister damage.

We assume further that the water flow in the disturbed zone is so large that any equivalent film resistance to the uptake of nuclides in the flowing water is negligible, but can easily be added in the same manner as before.

With these assumptions we can define a diffusion resistance occurring in the backfill extending from the plane mentioned above in level with the top of the canister to the level of the "disturbed zone". The value of this resistance, R_{CDist}, is calculated from eq (2) as

$$R_{CDist} = \frac{\phi}{\pi \cdot r_2^2 \cdot D_C} \tag{45}$$

where ϕ is the distance from the top of the canister to the disturbed zone.

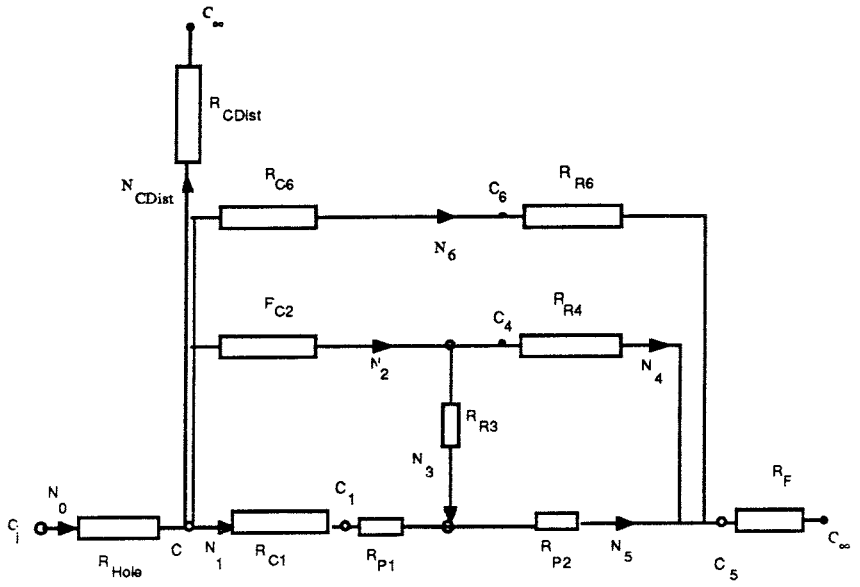

Figure 13. Resistance network with transport route to the disturbed zone added.

The resistance, defined in this way, only takes into account the diffusion resistance in the clay above the canister top, implying that the damage would be placed on or very close to the top, resulting in a very conservative estimation of the backfill resistance if the damage were situated further down on the canister. This resistance is then coupled to the resistance network at a point between the resistance in the canister damage (R_{Hole} or R_{Rupt}) and the initial basic network, as shown in figure 13.

In the equation system this resistance is incorporated as coupled in parallel with the initial basic network since the end points of the basic network and the route to the disturbed zone have the same potential, C_{∞}, although they are not physically the same points.

This transport route can subsequently easily be expanded to incorporate transport into the tunnel sand/bentonite filling and further into fractures intersecting the tunnel.

4 EQUATION SYSTEM FOR THE RESISTANCE NETWORK

The resulting resistance of the whole network is resolved by a series of manipulations using the star-polygon rule and the Ohm's laws.

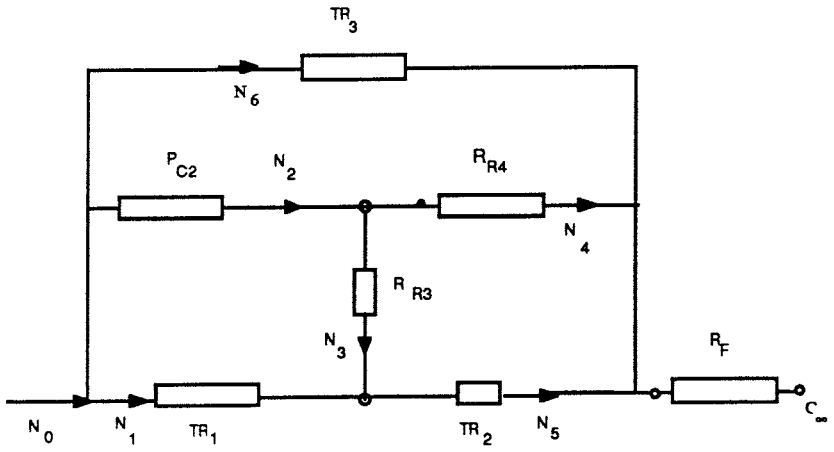

In setting up the equation system a number of help variables, TR_n, are used.

$$TR_1 = RC_1 + RP_1 \tag{46}$$

$$TR_2 = RP_2 \tag{47}$$

$$TR_3 = RC_6 + RR_6 \tag{48}$$

Using the star-polygon rule on the triangle TR_3-RC_2-RR_4 gives

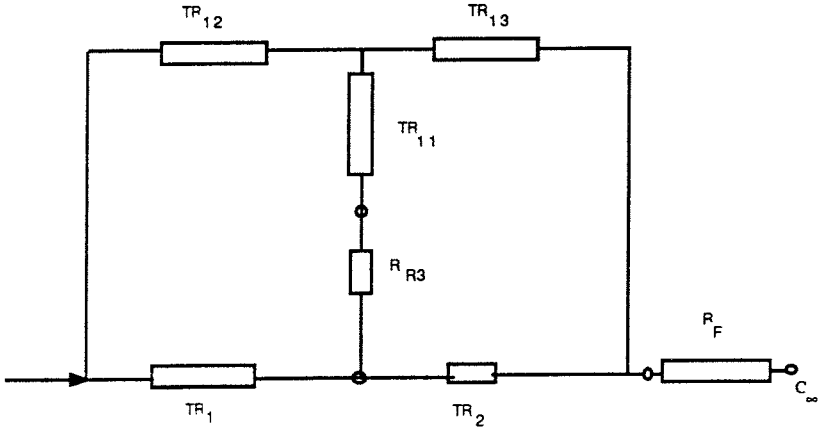

$$TR_{11} = \frac{RC_2 \cdot RR_4}{RC_2 + RR_4 + TR_3} \tag{49}$$

$$TR_{12} = \frac{RC_2 \cdot TR_3}{RC_2 + RR_4 + TR_3} \tag{50}$$

and

$$TR_{13} = \frac{RR_4 \cdot TR_3}{RC_2 + RR_4 + TR_3} \tag{51}$$

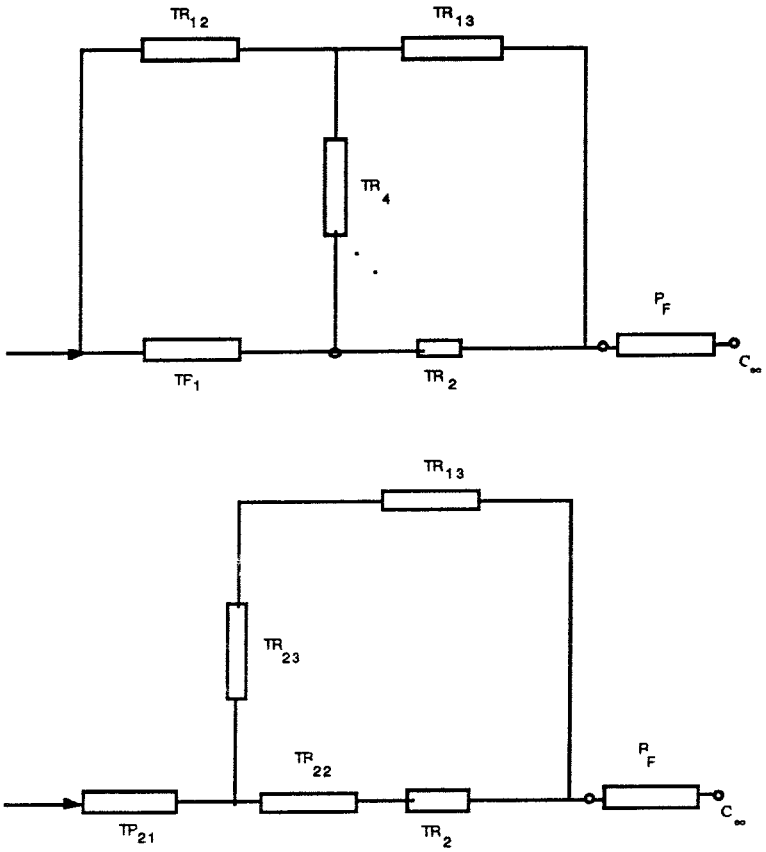

If then $TR_4 = TR_{11} + RR_3$, the the star-polygon rule can be used on the triangle TR_1-TR_{12}-TR_4 yielding

$$TR_{21} = \frac{TR_1 \cdot TR_{12}}{TR_1 + TR_{12} + TR_4} \tag{52}$$

$$TR_{22} = \frac{TR_1 \cdot TR_4}{TR_1 + TR_{12} + TR_4} \tag{53}$$

$$TR_{23} = \frac{TR_{12} \cdot TR_4}{TR_1 + TR_{12} + TR_4} \tag{54}$$

leaving us with (TR23+TR13) and (TR22+TR2) coupled in parallel

$$TR_5 = \frac{(TR_{23} + TR_{13}) \cdot (TR_{22} + TR_2)}{TR_{23} + TR_{13} + TR_{22} + TR_2} \tag{55}$$

and the resulting resistance

$$RRES = TR_{21} + TR_5 + RF \tag{56}$$

Thus we get the total equivalent flow rate in the sector as

$$N_0 = \frac{(C_0 - C_\infty)}{RRES} \quad \text{or if} \quad C_\infty = 0 \text{ and } C_0 = 1 \tag{57}$$

$$Q_{eq0} = N_0 = \frac{1}{RRES} \tag{58}$$

The equation system for solving the flow rate through the different routes then becomes

$$N_0 = N_1 + N_2 + N_6 \tag{59}$$

$$N_5 = N_1 + N_2 - N_4 \tag{60}$$

$$N_2 = N_3 + N_4 \tag{61}$$

$$N_1 \cdot TR_1 + N_5 \cdot TR_2 = N_2 \cdot RC_2 + N_4 \cdot RR_4 \tag{62}$$

$$N_1 \cdot TR_1 + N_5 \cdot TR_2 = N_6 \cdot TR_3 \tag{63}$$

$$N_1 \cdot TR_1 = N_2 \cdot RC_2 + N_3 \cdot RR_3 \tag{64}$$

and the concentrations along the backfill-rock interface become

$$\frac{C_1}{C_0} = 1 - N_1 \cdot RC_1 \tag{65}$$

$$\frac{C_2}{C_0} = 1 - N_2 \cdot RC_2 \text{ and} \tag{66}$$

$$\frac{C_6}{C_0} = 1 - N_6 \cdot RC_6 \tag{67}$$

and finally the concentration at the interface between the clay plug and the liquid film

$$\frac{C_5}{C_0} = (N_4 + N_5 + N_6) \cdot RF \tag{68}$$

5 RESULTS

The calculations are done in two parts. First the resistance network modelling the case with the entire canister wall corroded is solved, and a number of simulations are done. The results from these calculations are presented in figures 14 to 25 and compared with corresponding calculations made with a 3–D model of the same system. Simulation data for the models with a hole in the canister wall, a ruptured canister and influence from transport to the disturbed zone are then calculated from the results from the calculations of the first case.

The equation system has been solved for the following set of data:

Table 2. Fracture data used in calculations

Fracture aperture	$\delta = 10^{-3} - 10^{-4}$ m
Fracture spacing	$s = 2 \cdot d = 1, 10$ m
Clay plug penetration	$\sigma = 10^{-4}, 10^{-3}, 10^{-2}, 0.1, 0.5$ m
Water flow rate in rock	$u_o = 10^{-4}$ m^3/m^2,a
Canister hole diameter	$\lambda = 2.5 \cdot 10^{-3}$ m (hole area = 5 mm^2)
Canister fracture aperture	$\gamma = 10^{-4} - 10^{-2}$ m
Distance from top of canister to disturbed zone	$\eta = 1.5$ m

5.1 Calculations for model with completely corroded canister

The results can be studied in figures 14 - 17 , where the equivalent flow rates are given vs the plug lengths (σ). As a reference value is shown the equivalent flow rate that would arise if all resistances except the backfill resistance would be set at zero, corresponding to a hypothetical case where the canister , surrounded by compacted bentonite is suspended in an infinite volume of water, flowing past the canister with very high velocity, i.e. no film resistance. The mass transfer resistance for this reference case will then be

$$R_{ref} = \frac{\ln \frac{r_2}{r_1}}{\pi \cdot s \cdot D_C} \tag{69}$$

which with s = 1 m gives R_{ref} = 5.52·10^9 s/m^3. This corresponds to an equivalent flow rate,
$Q_{eq,ref}$ = 3.717 l/a,m or 18.6 l/a,canister.

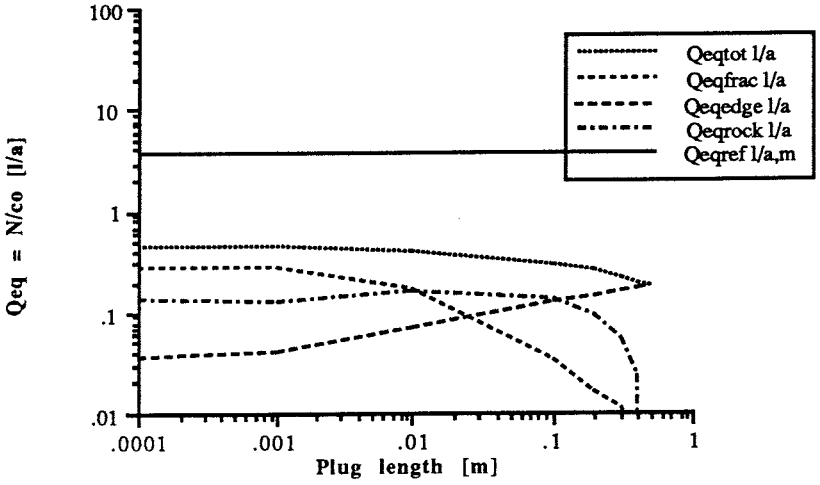

Figure 14. Resistance network model, completely corroded canister. Equivalent flow rate per fracture at backfill/rock interface. Fracture spacing 1 m, fracture aperture 0.1 mm

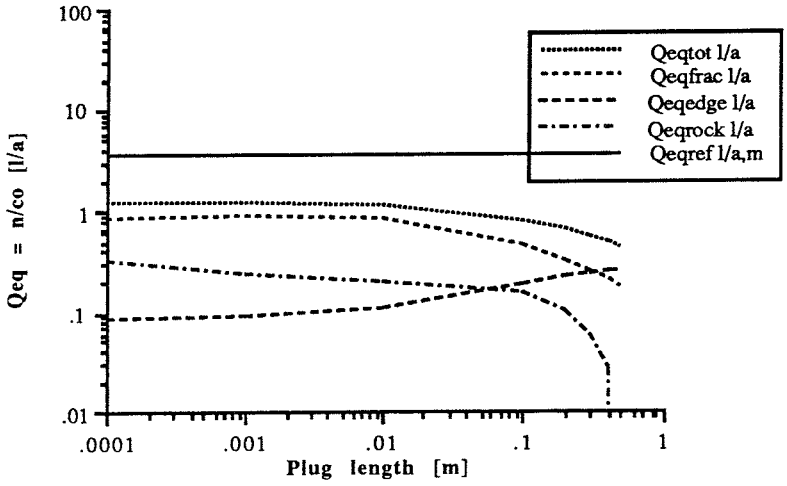

Figure 15. Resistance network model, completely corroded canister. Equivalent flow rate per fracture at backfill/rock interface. Fracture spacing 1 m, fracture aperture 1 mm

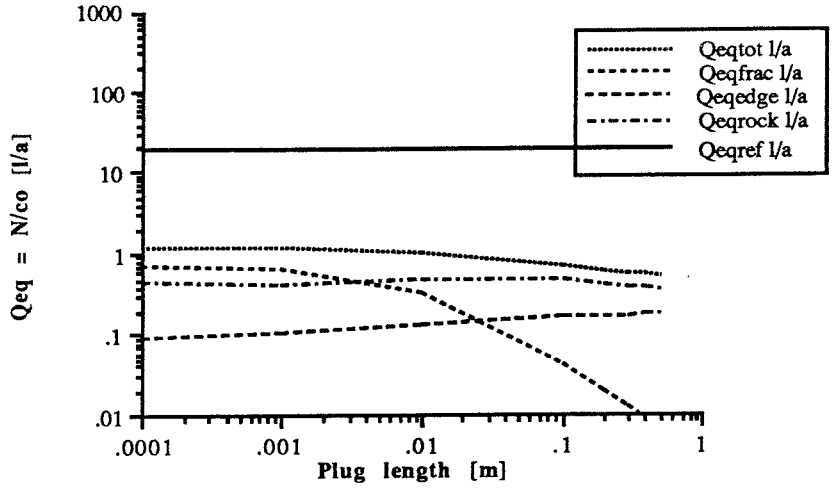

Figure 16. Resistance network model, completely corroded canister. Equivalent flow rate per fracture at backfill/rock interface. Fracture spacing 10 m, fracture aperture 0.1 mm

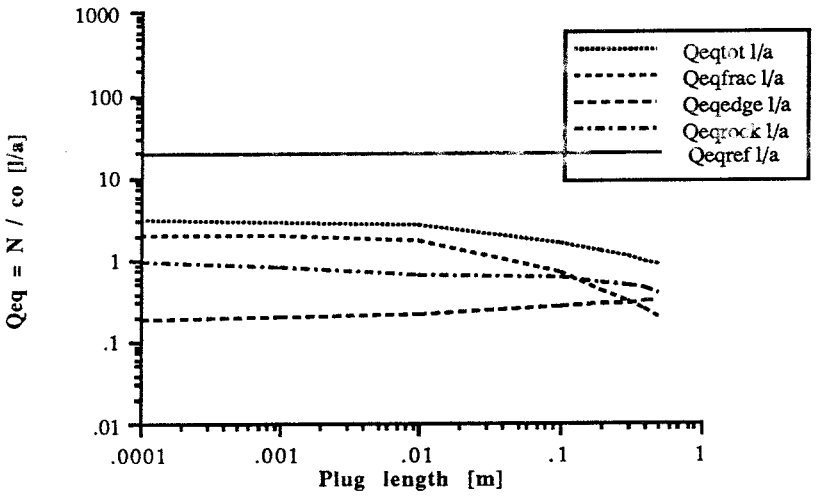

Figure 17. Resistance network model, completely corroded canister. Equivalent flow rate per fracture at backfill/rock interface. Fracture spacing 10 m, fracture aperture 1 mm

The general conclusion that can be drawn from these Figures is that in all cases the film resistance is the dominating diffusion barrier and that a penetration of clay into the fracture mouth only has limited influence on the total flow rate of nuclides in the system. Regardless of the length of the plug penetration the flow rate through the rock paths (edge and rock matrix) will be of the same

order of magnitude. The plug only influences the flow rate through the fracture mouth.

If we relate the equivalent flow rates along the respective paths to the total equivalent flow rate, as in figures 18-21, we can see that the contribution to the total flow rate via the fracture dominates as long as the ratio of the penetration length of the clay plug to the fracture aperture is in the order of 100 or less, regardless of fracture spacing.

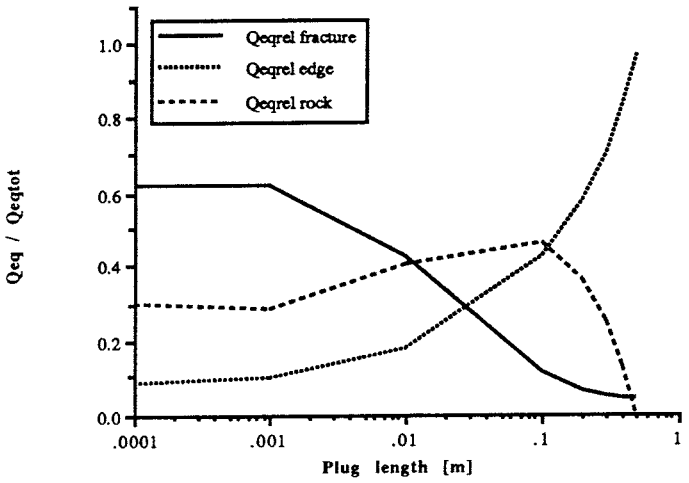

Figure 18. Relative equivalent flow rates at backfill/rock interface vs plug length. Fracture spacing 1 m, fracture aperture 0.1 mm.

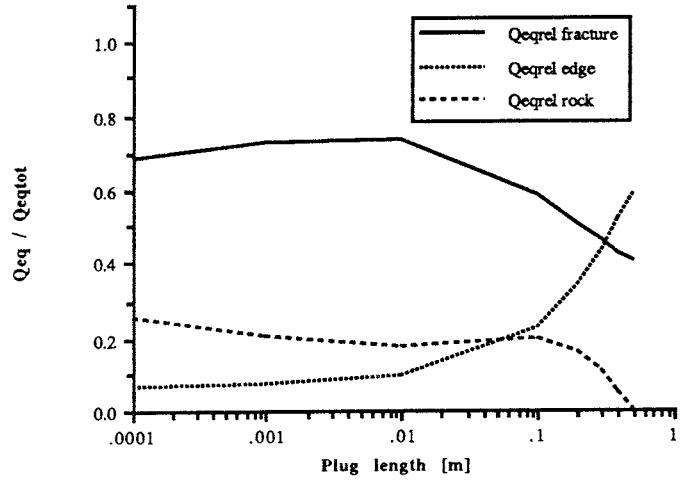

Figure 19. Relative equivalent flow rates at backfill/rock interface vs plug length. Fracture spacing 1 m, fracture aperture 1 mm.

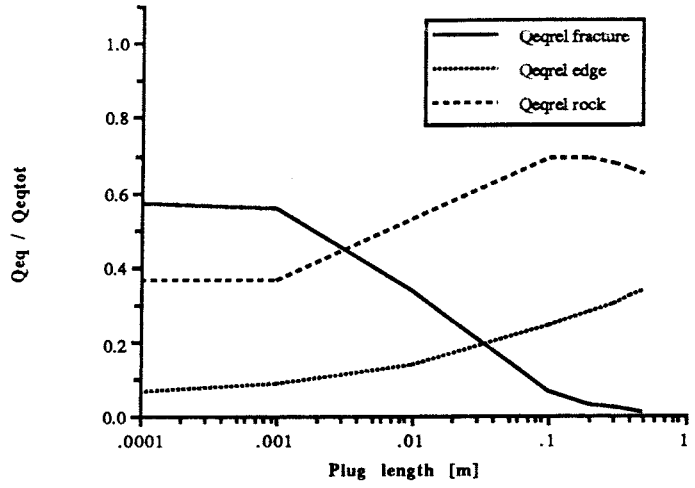

Figure 20. Relative equivalent flow rates at backfill/rock interface vs plug length. Fracture spacing 10 m, fracture aperture 0.1 mm.

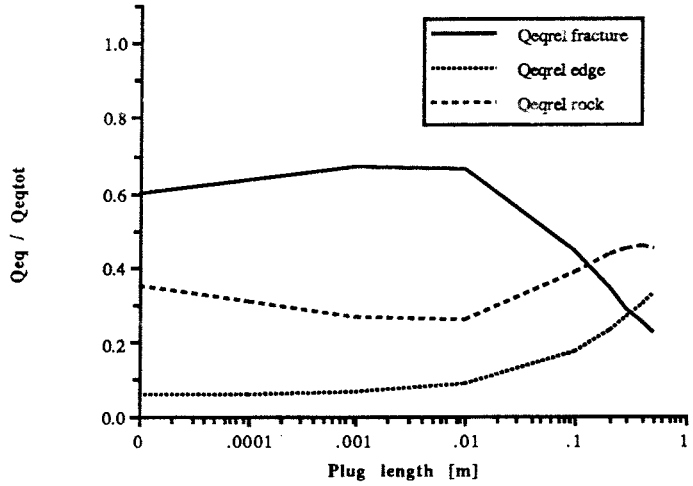

Figure 21. Relative equivalent flow rates at backfill/rock interface vs plug length. Fracture spacing 10 m, fracture aperture 1 mm.

In figures 22 and 23 the concentration profiles at the backfill/rock interface are presented for two different sets of parameters. In figure 22 we can see how the concentration varies for different fracture geometries, and in figure 23 for different penetration lengths of the clay plug. From these figures it is obvious that the concentration in the backfill deviates from a value of c/co=1 only in an area very close to the fracture mouth.

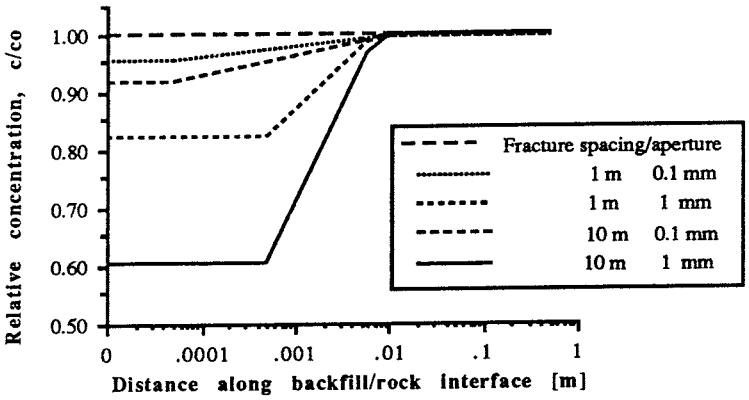

Figure 22. Concentration profile along the backfill/rock interface for different fracture geometries. Clay plug penetrating 10 mm into fracture.

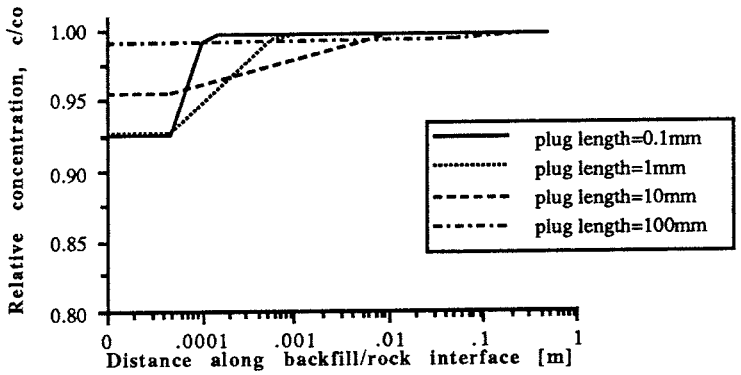

Figure 23. Concentration profile along backfill/rock interface vs plug penetration. Fracture spacing 1 m, fracture aperture 0.1 mm

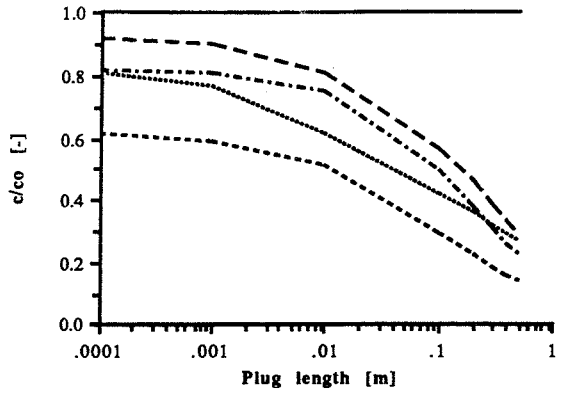

(a)

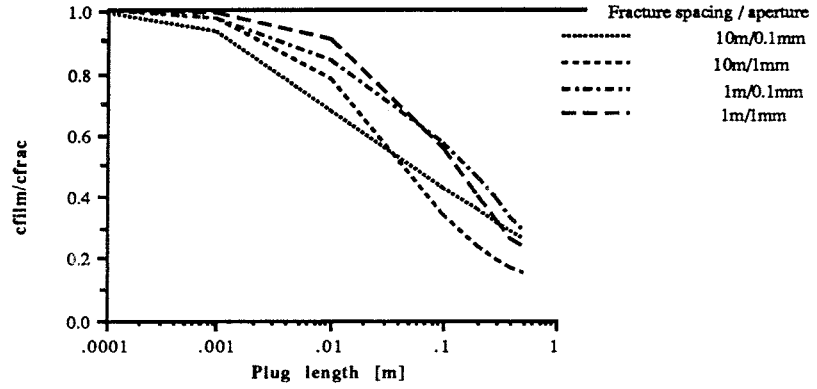

(b)

Figure 24a & b. Concentration profiles at the clay plug/fracture water interface vs plug penetration for different fracture geometries.

Figure 24a shows the concentration at the interface between the clay plug and the flowing water in the fracture. Figure 24b shows the relation between the contribution to the equivalent flow rate by the clay plug and the equivalent film resistance in the flowing water. The area below the curves represents the influence from the film resistance and the area between the curves and the line with the ordinate value = 1.0 that of the clay plug.

As a summary of the calculated data for different fracture geometries and plug lengths the total equivalent flow rate per fracture and per entire canister is presented in figures 25a and 25b respectively.

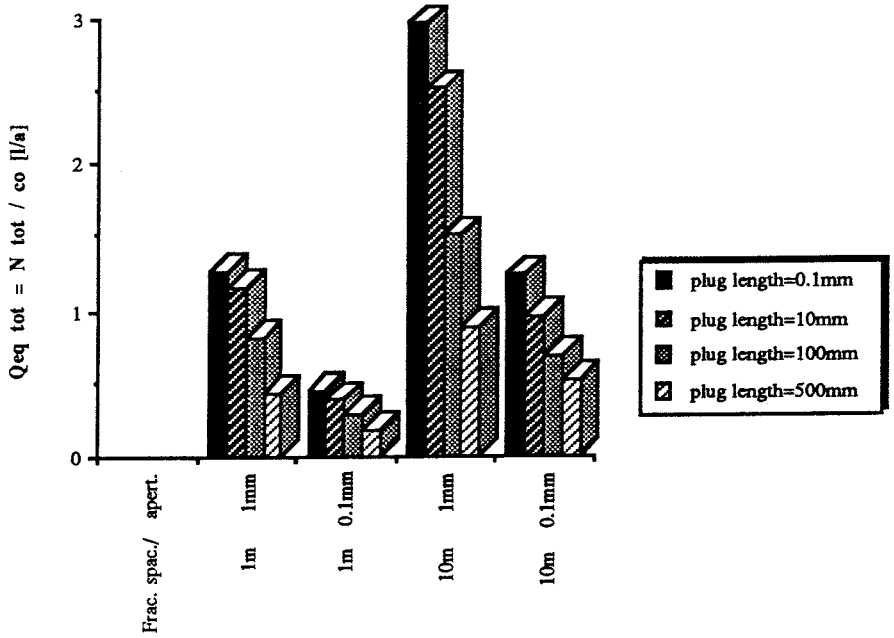

Figure 25a. Total equivalent flow rate per fracture for different fracture geometries and plug lengths

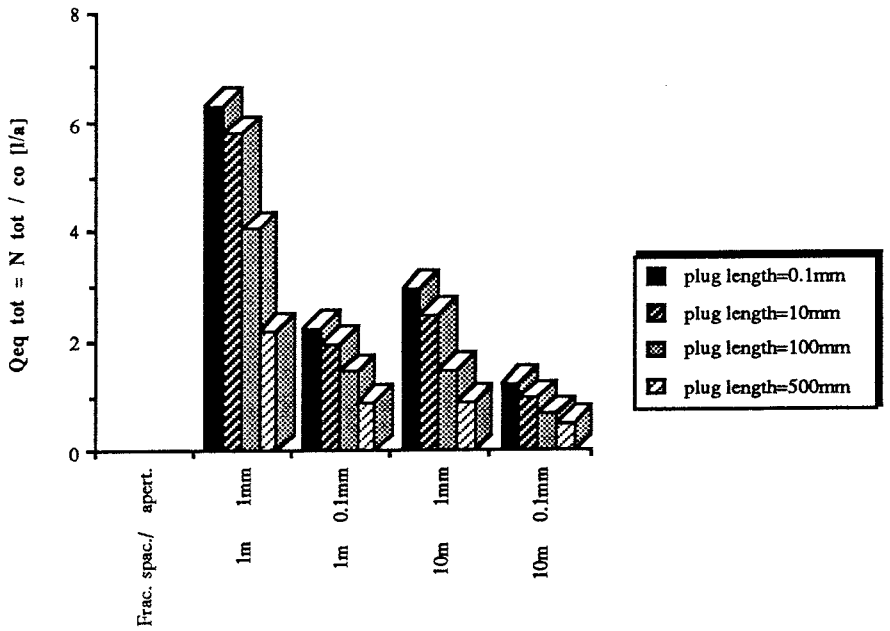

Figure 25b. Total equivalent flow rate per canister for different fracture geometries and plug lengths

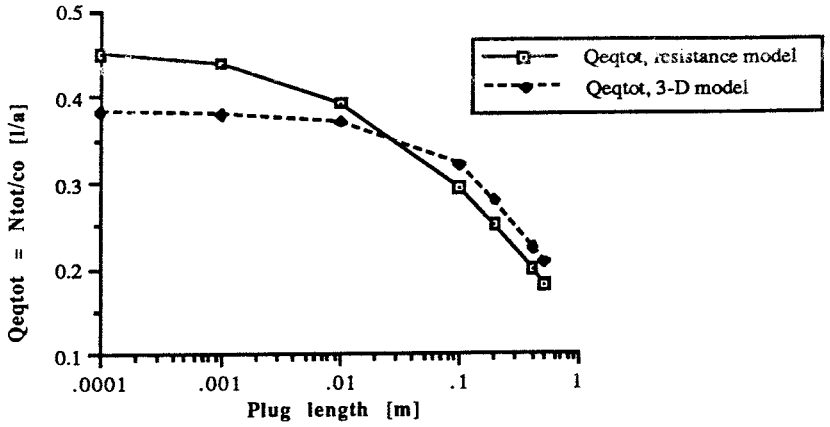

Figure 26. Comparison of the 3-D numerical model and the resistance network model. Total equivalent flow rates in a single fracture. Fracture spacing 1 m, fracture aperture 0.1 mm.

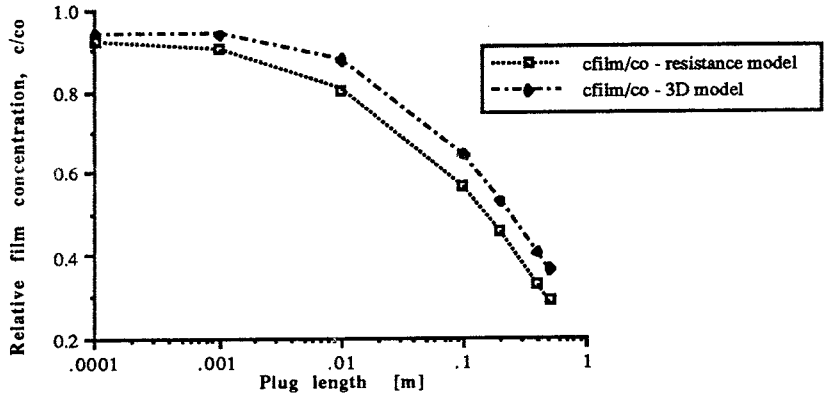

Figure 27. Comparison of the 3-D numerical model and the resistance network model. Relative concentration at the clay plug / fracture water interface. Fracture spacing 1 m, fracture aperture 0.1 mm.

In order to validate the resistance network model comparison has been made between the above presented simulation results and results obtained from simulations made with a 3-D numerical method (App II) for a central data set, i.e. with a fracture spacing of 1 m and a fracture aperture of 0.1 mm. The comparison is presented in figures 26 and 27. From these can be seen that the correlation between the two methods is very good.

5.2 Calculations for the model with a hole in the canister wall

If the damage to the canister is restricted to a single hole instead of the entire wall being corroded the basic resistance network is amended as shown in figure 11 simply by adding a resistance, R_{Hole}, in series with the initial network. This resistance is calculated using the equation

$$R_{Hole}=\frac{1}{\pi\cdot\lambda}\cdot\left(\frac{4\cdot t}{\lambda\cdot D_W}+\frac{1}{D_C}\right) \qquad (40b)$$

Assuming that the damage to the canister is caused by a fabrication error during the welding of the canister not detected at the final inspection, the size of the hole has to be very small. We assume that the area of the hole is 5 mm^2 corresponding to a diameter (λ) of $2.5\cdot10^{-3}$ m.

The equivalent resistance to the nuclide diffusion for this case thus becomes $R_{Hole}= 2.00\cdot10^{5}$ a/m^3 corresponding to an equivalent flow rate contribution of $Q_{eqHole}= 5.0\cdot10^{-3}$ l/a.

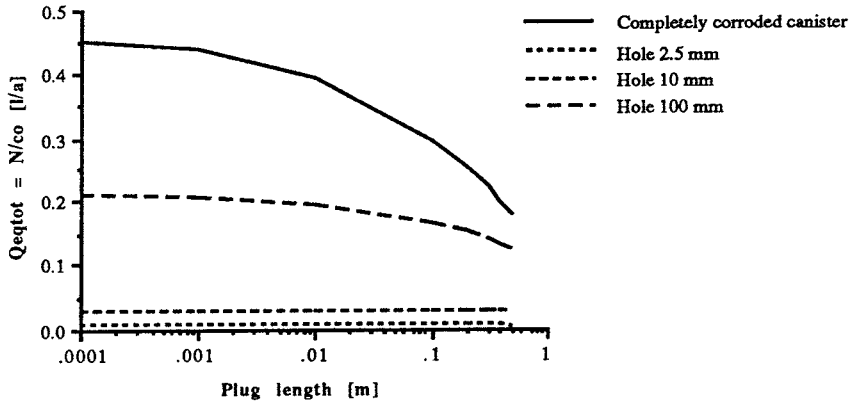

Figure 28. Comparison between completely corroded canister and holes in the canister wall. Total equivalent flow rates per fracture. Fracture spacing 1 m, aperture 0.1 mm.

The total equivalent flow rate will therefore be dominated by the resistance in the hole, as can be seen in figure 28 where the total equivalent flow rate into a single fracture with the canister wall completely corroded is compared with the resulting flow rate from a hole in the wall, with hole diameters varying from 2.5 to 100 mm.

5.3 Calculations for the model with a slit in the canister wall

If the damage to the canister as described in chapter 3.4 is caused by a shearing of the canister resulting in a fracture extending around the entire canister the basic resistance network is amended in the same way as was done for the case with a hole in the canister wall, by adding a resistance, R_{Rupt} to the initial network. his resistance is calculated with the equation

$$R_{Rupt} = \frac{1}{2 \cdot \pi \cdot r_1} \cdot \left(\frac{t}{\gamma \cdot D_W} + \frac{4}{D_C} \right) \qquad (44)$$

As in the case of a hole in the canister wall, the entry resistance, R_{SC}, is independent of the size of the canister damage. The value of this resistance becomes $R_{SC} = 1.34 \cdot 10^3$ a/m^3, corresponding to an equivalent flow rate contri-bution of $Q_{eqSC} = 0.74$ l/a. The influence of the fracture itself, will as in the case with the hole be quite substantial, for fracture apertures of about 1 mm and less.

Depending on the nature and severity of the shearing action on the canister the aperture of the canister fracture can vary within wide limits, however if the fracture would open by more than a few centimeters the probability of a simultaneous dislocation of the canister parts would be so large that a completely new set of boundary conditions would have to be applied.

The influence on the total equivalent flow rate of nuclides from a fractured canister is presented in figure 29.

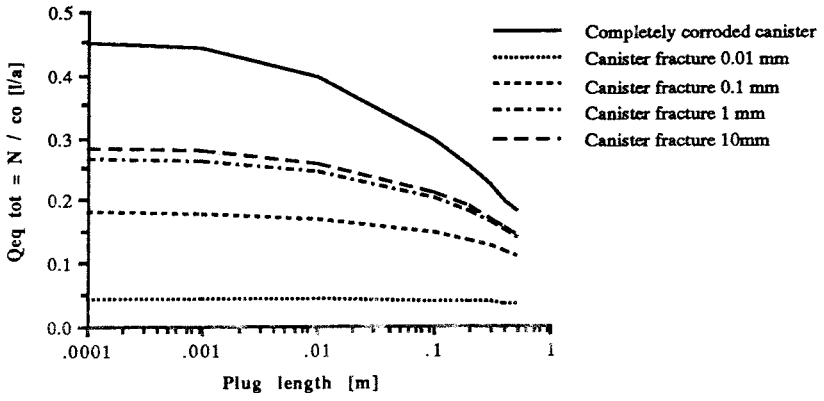

Figure 29. Comparison of completely corroded canister and fractures in the canister wall. Total equivalent flow rates per fracture.
Fracture spacing 1 m, rock fracture aperture 0.1 mm.

5.4 Calculations for model combined with transport to the disturbed zone

In order to incorporate the transport of nuclides from the damaged canister up through the backfill in the repository hole to the disturbed zone adjacent to the transport tunnel a resistance

$$R_{CDist} = \frac{\phi}{\pi \cdot r_2^2 \cdot D_C} \tag{45}$$

is connected to the network model at a point between the resistance in the canister damage and the initial basic network.

The distance between the top of the canister and the disturbed zone is set to 1.5 m and with a repository hole radius $r_2 = 0.75$ m and the backfill diffusivity $D_C = 4 \cdot 10^{-11}$ m^2/s the resistance is $R_{CDist} = 0.67 \cdot 10^3$ a/m^3.This corresponds to an equivalent flow rate contribution of $Q_{eqCDist}$ =1.49 l/a per canister.

Figure 30 shows the influence of the disturbed zone on the total equivalent flow rate in the diffusion system of the uppermost fracture for the central fracture geometry case. It is reasonable to assume that the flow path to the disturbed zone won't influence the flow rate to lower situated fractures.

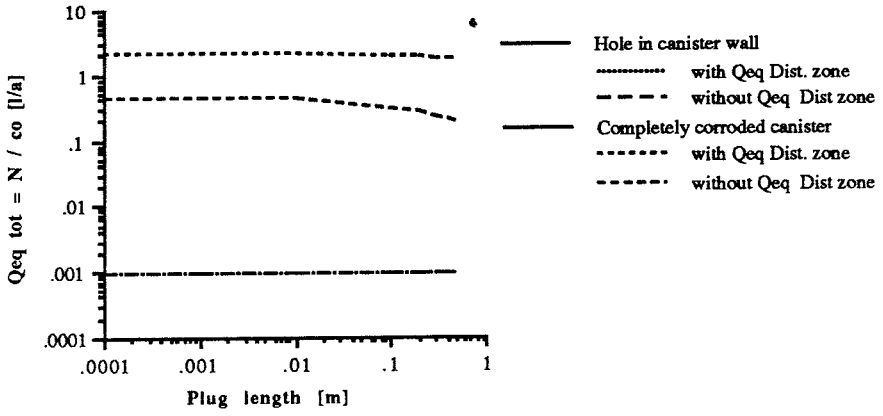

Figure 30. Influence of flow path to the disturbed zone on the total equivalent flow rate in the diffusion system of the uppermost fracture. Fracture spacing 1 m, fracture aperture 0.1 mm

The diagram shows that the disturbed zone has a marked effect for the case with a completely corroded canister but for a case with a localized damage to the canister wall the influence from the disturbed zone is barely marginal.

6 CONCLUSIONS

A model has been developed describing the diffusion pattern of radionuclides released from a damaged canister in the near field of a repository for spent nuclear fuel. The model is based on a network of mass transfer resistances coupled together in the same way as an electrical circuit network. The equations used to describe the network are consequently based on laws normally used in Electrical Engineering. The resulting equation system consists throughout of simple linear equations, so the system is very simple and fast to solve using conventional methods.

Initially a basic network describing the transport from a completely corroded canister, through the backfill of compacted bentonite clay surrounding the canister and into a fracture dissecting the repository hole is presented. It is assumed that the backfill clay will penetrate a short distance into the fracture. From the backfill nuclides enter the fracture via a number of transport routes leading directly into the fracture mouth or through the rock matrix.

This basic network model is subsequently expanded to cover other types of damage to the canister, fabrication damage or localized corrosion resulting in a hole of limited size in the canister wall and shearing of the canister resulting in a fracture in the canister wall. To the model is also added a transport route leading to the so called "disturbed zone" around the transport tunnel in which the repository is located.

Simulations made using the model are compared with calculations for the same system using a 3-dimensional numerical solution model. This comparison shows a very good agreement between the two models. The resistance network model is vastly more simple to use and to modify than the 3 dimensional numerical model.

The conclusion that can be drawn from the results of the simulation calculations is that the resistance network model developed in this report offers a simulation tool with large flexibility and very short calculation time compared to other more complex models without loosing significant accuracy and validity. The model can easily be expanded to incorporate additional transport paths.

7 NOTATIONS

A	Diffusion area	[m^2]
a	thickness of the backfill	[m]
b	distance far away (along x-axis)	[m]
c_0	concentration of radionuclides at the surface of the canister	[mol/m^3]
c_i	concentration of radionuclides	[mol/m^3]
C	dimensionless concentration	[-]
d	half distance between fractures (s/2)	[m]
D_i	effective diffusivity	[m^2/s]
k_i	mass transfer coefficient	[m^3/m^2,a]
N	mass flow of radionuclides	[mol/a]
Q	equivalent volumetric flow rate (=N/c_0)	[m^3/a]
r_i	radius from center of the hole	[m]
R_i	resistance to flow	[a/m^3]
s	distance between fractures	[m]
t_r	contact time	[a]
t	thickness of canister wall	[m]
TR_n	help variables	
u_0	Darcy velocity (flux)	[m^3/m^2,a]
u_F	water velocity in the fracture	[m/a]
W	width of the block	[m]
w	width of a channel	[m]
x_i	distance along the x-axis	[m]
y_i	distance along the y-axis	[m]
β, ν	y-coordinates for the general solution of the diffusion equation	[-]
δ	aperture of the fracture	[m]
ε	effective porosity	[-]
η	error function parameter	
ϕ	distance from top of canister to the disturbed zone	[m]
λ	diameter of the hole in the canister wall (case 2)	[m]
γ	aperture of a fracture in the canister wall	[m]
σ	penetration of clay plug into the fracture	[m]
τ	tortuosity	[-]
ζ	channel division fraction	[-]
θ	angle of enclosure	[rad]

8 REFERENCES

Anderson, G., A Rasmuson, and I. Neretnieks,
"Migration Model for the Near Field: Final Report", KBS TR 82-24 1982

Bird, R.B., Stewart, W.E. and Lightfoot, E.N., Transport Phenomena, Wiley & Sons 1960.

KBS-3, "Final Storage of Spent Nuclear Fuel",
Swedish Nuclear Fuel Supply Co., Division KBS May 1983.

Lee H.S., Moreno, L., Neretnieks, I., Nilson L., "An Estimation of Nuclide Release Rate Rear The Canister (Near Field Model 91), KBS TR 89-38 1989

Özisik,M.N., Mikhailov M.D., "Unified Analysis and Solutions of Heat and Mass Diffusion" John Wiley & Sons, 1984)

Neretnieks, I., "Transport of Oxidants and Radionuclides through a Clay Barrier", KBS TR 79 1978

Neretnieks, I., "Transport Mechanisms and rates of Transport of Radionuclides in the Geosphere as Related to the Swedish KBS Concept." Proceedings of Symposium. Underground Disposal of Radioactive Wastes IAEA/NEA, Vienna 1980, Vol 2, p. 315

Neretnieks, I., "The Movement of a Redox Front Downstream from a Repository for Nuclear Waste", Nucl. Techn. 62, July 1983, p 110.

Neretnieks, I., "Stationary Transport of Dissolved Species in the Backfill Surrounding a Waste Canister in Fissured Rock: Some Simple Analytical Solutions", Nuclear Technology, 72, 194 1986

Pigford, T.H.G., Chambré P.L., Lee, W.W.-L., "A Review of Near Field Mass Transfer in Geologic Disposal Systems", Lawrence Berkeley Laboratory, Univ. of Calif., Earth Sciences Div., Report LBL-27045, Feb. 1990.

Appendix I.
DATA USED IN CALCULATIONS

Table 3. Data used in calculations

Backfill diffusivity	$D_C = 4 \cdot 10^{-11}$	[m^2/s]
Clay plug diffusivity	$D_P = 4 \cdot 10^{-10}$	[-"-]
Rock diffusivity	$D_R = 7{,}4 \cdot 10^{-13}$	[-"-]
Water diffusivity	$D_W = 3.9 \cdot 10^{-9}$	[-"-]
Canister radius	$r_1 = 0.375$	[m]
Radius of repository hole	$r_2 = 0.75$	[m]
Width of parallel-epiped	$W = 1$	[m]
Envelope angle at which the film resistance is calculated	$\Omega = \pi/4$	[rad]
Fracture aperture	$\delta = 10^{-3} - 10^{-4}$	[m]
Fracture spacing	$s = 2 \cdot d = 1, 10$	[m]
Clay plug penetration	$\sigma = 10^{-4}, 10^{-3}, 10^{-2}, 0.1, 0.5$	[m]
Water flux in rock	$u_o = 10^{-4}$	[m^3/m^2,a]
Canister hole diameter	$\lambda = 2.5 \cdot 10^{-3}$	[m](hole area = 5 mm^2)
Canister fracture aperture	$\gamma = 10^{-4} - 10^{-2}$	[m]
Distance from top of canister to disturbed zone	$\eta = 1.5$	[m]

Appendix II

2 & 3-D CALCULATIONS TO VALIDATE THE RESISTOR MODEL

In order to compare and validate the results of the simulations made with the resistance network model a numerical solution is made of the transport of radionuclides from a totally corroded canister is developed using the same geometric model as that described in chapter 2.

The cylindrical geometry of the system, canister-backfill-rock, is simplified and transformed to a system of rectangular geometry as in SKB 89-38 (Lee et al., 1989)

The calculations are performed for a system in steady state for radionuclides of very long half-life. The nuclide concentration at the wall of the canister is assumed to be constant. The backfill layer is assumed to be sufficiently impermeable to the water flow to render the liquid in the backfill pores to be stagnant.

Radionuclides diffuse from the canister into and through the backfill, continuing both through the porous rock and through the mouth of the fracture to reach the flowing water in the fracture.

Within the fracture in the sector around the hole, the diffusion of radionuclides from all the directions and the water flowing around this sector contribute to build up a concentration profile.

The mechanisms of transport considered in the model are diffusion through the solid material (bentonite, plug and rock) and advection plus diffusion in the fracture.

Figure 31 shows a schematic view around the canister with the mouth of the fracture plugged by backfill (rectangular coordinates are used as discussed above). Radionuclides may reach the flowing water by

- diffusing through the backfill to the fracture mouth, then through the plug in the fracture into the flowing water - path Q_1,
- diffusing through the backfill-porous rock, into the fracture - path Q_2.
- diffusing through the backfill, the rock, plug in the fracture, into the flowing water in the fracture - path Q_3.

The model was solved for a 3-D system. This solution is very computer time consuming. Also a 2-D solution was developed.

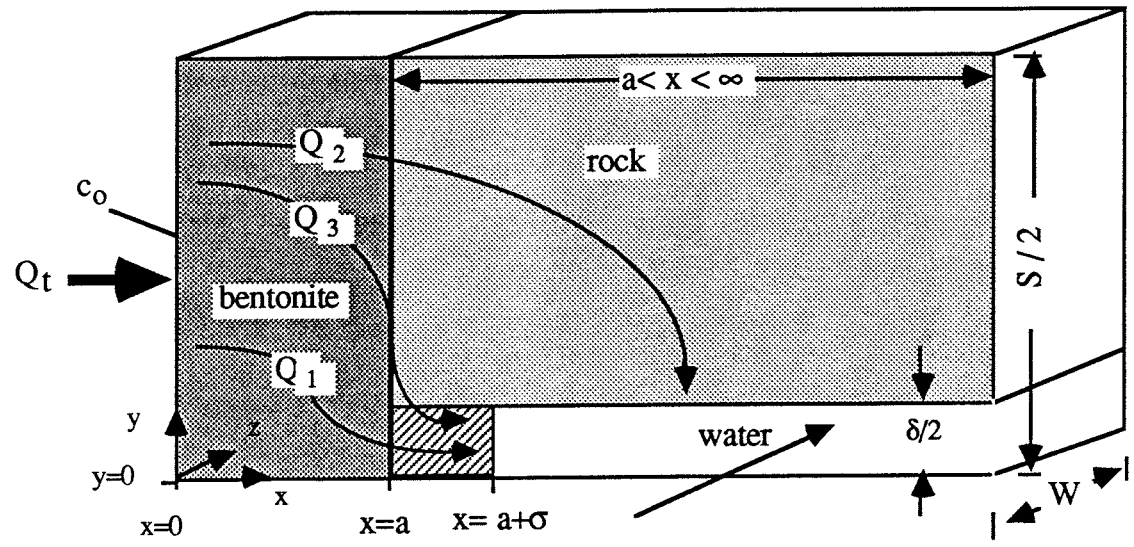

Figure 31. Simplified schematic view near the canister when the fracture is plugged a length σ with bentonite. The mouth of the fracture is open to the diffusion of radionuclides.

II.1 Mathematical model, 3-D

It is noted that the radionuclide concentration will be changing in all three directions in the Cartesian system. The water flow is in the z-direction simulating the water flowing around the hole.

The governing equations for the different solid-materials and the flowing water in the fracture may be obtained from Table 18.2-2. (Bird et al., 1960). Assuming that the densities and diffusivities for the solid materials are constant and that the water is flowing in the z-direction, i.e. $v_y = v_x = 0$,

The governing equation for transport in the solid regions is

$$\nabla^2 c_A = 0 \tag{70}$$

The governing equation for the fracture including diffusion from the rock and from the plug into the flowing water and the fluid transport (advection) along

the fracture, parallel to the surface of the interface backfill-rock

$$-D_w \nabla^2 c_A + v \cdot \nabla c_A = 0 \tag{71}$$

The boundary conditions are expressed as follows

- at the canister surface, plane x = 0, the concentration.is constant

$$c = c_0 \qquad \text{for } 0 < y < \frac{s}{2}, \quad 0 < z < W \tag{72}$$

- there is no flux across the planes at y = 0 and y = s/2 (symmetric assumption).

$$\left.\frac{\partial c}{\partial y}\right|_{y=0} = 0 \qquad \text{for } 0 < x < \infty, \quad 0 < z < W \tag{73}$$

$$\left.\frac{\partial c}{\partial y}\right|_{y=s/2} = 0 \qquad \text{for } 0 < x < \infty, \quad 0 < z < W \tag{74}$$

- there is no flux across the planes z = 0 and z = W in the direction perpendicular to these boundaries, except in the fracture.

$$\left.\frac{\partial c}{\partial z}\right|_{z=0} = 0 \tag{75}$$

$$\left.\frac{\partial c}{\partial z}\right|_{z=s/2} = 0 \tag{76}$$

- at long distances away from the interface backfill-rock, x = ∞, the boundary condition is

$$\left.\frac{\partial c}{\partial x}\right|_{x=\infty} = 0 \qquad \text{for } \delta/2 < y < \frac{s}{2}, \quad 0 < z < W \tag{77}$$

II.2 Mathematical model, 2-D

The 3-D model is reduced to 2 dimensions by averaging the development of the concentration profile in the fracture water. By studying the results from the 3-D calculations one can deduce that an average value of the mass transfer resistance is reached when the concentration profile has been allowed to develop during 25% of the contact length along the fracture mouth, i.e. after an envelope angle of $\pi/4$.

In the 2-D model it is assumed that this average concentration profile is effective along the entire contact length.

In the x- and y-directions the geometry is symmetrical.

Calculations are done for different concentration profiles in the fracture. These profiles are calculated assuming a constant concentration at the fracture mouth and diffusion from the backfill into the flowing water.

In this case the boundary condition at the mouth of the fracture, $x= a+\sigma$, is that the concentration is constant.

$$c = c_1 \qquad \text{for} \quad 0 < y < \delta/2 \tag{78}$$

and along the wall of the fracture, at $y= \delta/2$, the concentration is

$$c = c_1 \, \text{erfc}\,(\eta) \qquad \text{for} \quad x > a + \sigma \tag{79}$$

where

$$\eta = \frac{x\text{-}a\text{-}\sigma}{\sqrt{4 D_w t_r}} \tag{80}$$

The contact time, t_r, is calculated as

$$t_r = \frac{f \pi r_2 \delta}{u_0 S} \tag{81}$$

where r_2 is the radius of the interface plug-water in the fracture measured from the center of the canister, D_w is the effective diffusivity of the free water, s is the space between fractures, u_0 is the Darcy velocity, and δ is the aperture of

the fracture. The factor f determines the location at which the concentration profile is calculated.

Two cases are considered:

- The fracture is free of backfill
- A part of the fracture is penetrated by the backfill, forming a plug.

The first case is a special case of the second one, where the length of the plug is zero or negligible.

II.3 Methodology of the solution

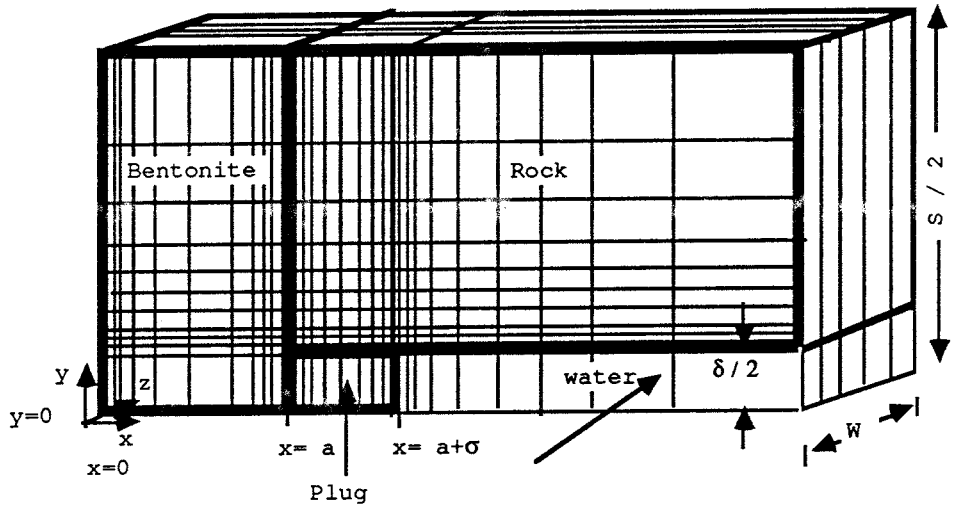

Figure 32. Schematic view of the geometric grid used in the computing of the release of radionuclides in 3-D. Not at scale.

The grid used is very fine in the nodes close to the interfaces (clay-rock, rock-water, clay-water) and increases in a geometrical way by a factor of about 1.5. Figure 32 shows a view of the discretization used in the direction perpendicular to the water flow. In the direction of the water flow, a equidistant discretization is used. This means that the number of nodes is quite large. For a typical grid the dimensions are 55x20x20 nodes (22 000 nodes).

The governing equation (70) with the respective boundary conditions was numerically solved by using the IFDM (Integral Finite Differential Method) calculating the material balance for each node. The flow of radionuclides by diffusion, except in the fracture, at any direction may be calculated by Fick's law

$$N = -D\,A\,\frac{\Delta c}{\Delta L} \tag{82}$$

where ΔL is the diffusion length in the grid node.

The equivalent volumetric flow rate, Q, may be used to express the flow of contaminants, N. The equivalent flow rate is defined as the volume of solution with concentration c_o per time unit that would be generated by a contaminant flow of N moles per time unit. (Neretnieks, 1978)

$$Q = \frac{N}{c_o} = -D\,A\,\frac{\Delta\left(\frac{c}{c_o}\right)}{\Delta L} \tag{83}$$

where c is the concentration of the radionuclides, A is the diffusion area, and ΔL is the distance over which the driving force acts.

If we call "C" the dimensionless concentration defined as c/c_o, the transport of radionuclides by diffusion along, e.g. the x-axis, between two consecutive nodes with effective diffusion coefficients Di and Dj may be written as

$$Q_{i,j} = -\frac{C_j - C_i}{\frac{\Delta x_i}{2D_i\,\Delta y_i\,\Delta z_i} + \frac{\Delta x_j}{2D_j\,\Delta y_j\,\Delta z_j}} \tag{84}$$

If we call $R_{i,j}$, the resistance to flow between nodes i and j along the axis in particular

$$R_{i,j} = \left(\frac{\Delta x_i}{2D_i\,\Delta y_i\,\Delta z_i} + \frac{\Delta x_j}{2D_j\,\Delta y_j\,\Delta z_j}\right) \tag{85}$$

then

$$C_j - C_i = - Q_{i,j} R_{i,j} \tag{86}$$

Therefore, the mass balance for each node, i, may be written as

$$\sum_j Q_{ij} = \sum_j \frac{C_j - C_i}{R_{ij}} = 0 \tag{87}$$

When the water flow into the fracture in the z-direction is considered in the calculations, we get

$$Q|_z = \frac{N}{c_o}\Big|_z = -D \cdot A \frac{\Delta\left(\frac{c}{c_o}\right)}{\Delta z} + v \cdot c \tag{88}$$

The system of equations defined by equation (87) with the concentrations as unknowns is solved using a routine from the NAG library. The solution of the system of equations give the concentrations at each node, and the equivalent volumetric flow rate between adjacent nodes is calculated using equation (87).

II.4 Results and discussion

The geometric dimensions of the system, the water flow, and the effective diffusivities for the rock, bentonite, bentonite (plug), and free water are tabulated in Appendix I. The effective diffusivity for the bentonite used in plugging the fracture is assumed to be ten times larger than the effective diffusivity of the backfill. The flux (Darcy velocity) was assumed to be 0.1 l/(m^2.a).

The flow of radionuclides that reach the flowing water through different paths is calculated using the 2-D model. The calculations were performed for different spacings between fractures, different concentrations at the mouth of the fracture (c_1), different contact times, and different plug lengths. In the first set of calculations no plug in the fracture mouth was considered. In the second set different plug lengths in the fracture were used.

The 2-D model requires the assumption of a concentration in the fracture mouth. Moreover, the calculations are done for a given section (we have chosen $\pi/4$). The advantage of this approach is its short computing time compared to that obtained from the 3-D model. The 3-D model was used to solve a few cases which are taken as reference cases for the 2-D calculations and for the resistor model.

The values of the equivalent flow rate, Q_i, are related to an equivalent volumetric flow rate Q_0 equal to 1.15 l/a. This reference equivalent flow rate was calculated assuming zero concentration at the mouth of the fracture and no plug for a fracture aperture of 0.1 mm and a fracture spacing of 1 m.

II.4.1 Results, 2-D model

The 2-D model is solved for two cases, a) no plug in the fracture and b) with plug in the fracture.

The results from the 2-D model are calculated for different concentrations, c_1, at the mouth of the fracture. The imposed concentration profile within the fracture is calculated by equation 79.

From the 3-D model developed in a later stage in this report and also from the resistor model , was shown that the condition of concentration at the mouth of the fracture changes for any change introduces in the system as for example changes in the spacing between fracture, in the fracture aperture, in the plug length, etc. Then the release of radionuclides for any change introduced in the system, may be obtained if the new concentration condition is known. In this report, the release is obtained at the concentrations c_1 in the respective figures showing the results for the 2-D model.

II.4.1.1 Results for case without plug in the fracture

The 2-D model was used to test the influence of some parameters on the release of radionuclides into the flowing water. First we studied the influence of the contact time on the nuclide release, expressed as equivalent flow rate. The penetration length (or the shape) of the concentration profile in the fracture is determined by the contact time. Calculations were performed for contact times corresponding to envelope angles of $\pi/4$, $\pi/2$ and π (Equation 81).

The fraction of equivalent flow rate which flows directly into the fracture mouth (Q_1/Q_t) is slightly increased with the contact time for a given value of the concentration c_1. See Figure 33.

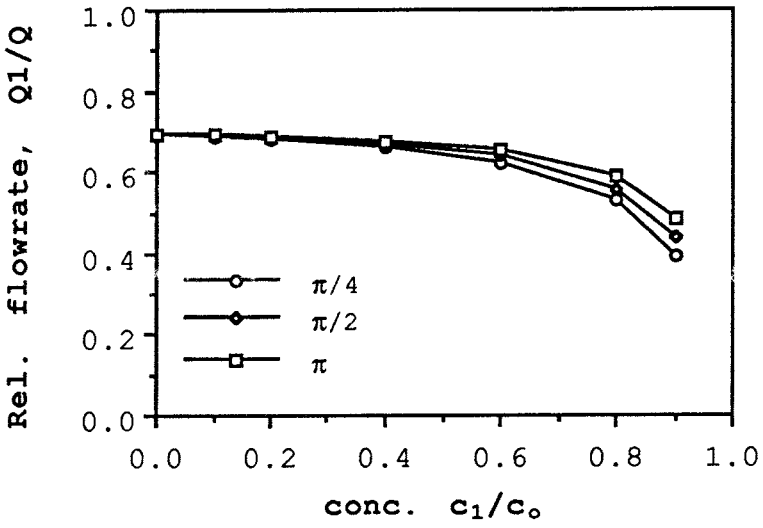

Figure 33. Flow rate dependency on the contact time and the dimensionless concentration at the mouth of the fracture c_1. For s = 1 m, and δ = 0.1 mm.

Calculations for different fracture spacings were made, and the results are shown in Figure 34. The release of radionuclides per fracture is increased by about 0.1 Q_0 when a fracture spacing of 5 m is used instead of 1 m for a given value of the concentration c_1. If the fracture spacing is increased, from 1 to 5 m, the water flow rate in the fracture is also increased in the same proportion. This means a decrease of the concentration in the fracture. The concentration at the fracture mouth was calculated by applying the simplified model (resistor model) for the release of contaminants. This model include an equivalent "film" resistance to take into account the diffusion in the flowing water in the

fracture. Values for these concentrations are plotted at Figure 34. The release per fracture decreases when a spacing of 1 m is used, for the case shown in Figure 34 this reduction is of about 60 %. If the equivalent flow rate (Q_t/Q_0) is related to the length of the canister (5 m), we get that the total release from the canister decreases when a larger spacing is used. The total release for the 5 fractures using a spacing of 1 m is about $1.0 \cdot Q_0$ ($5 \cdot 0.2 \cdot Q_0$) while that for a spacing of 5 m the total release is $0.38 \cdot Q_0$.

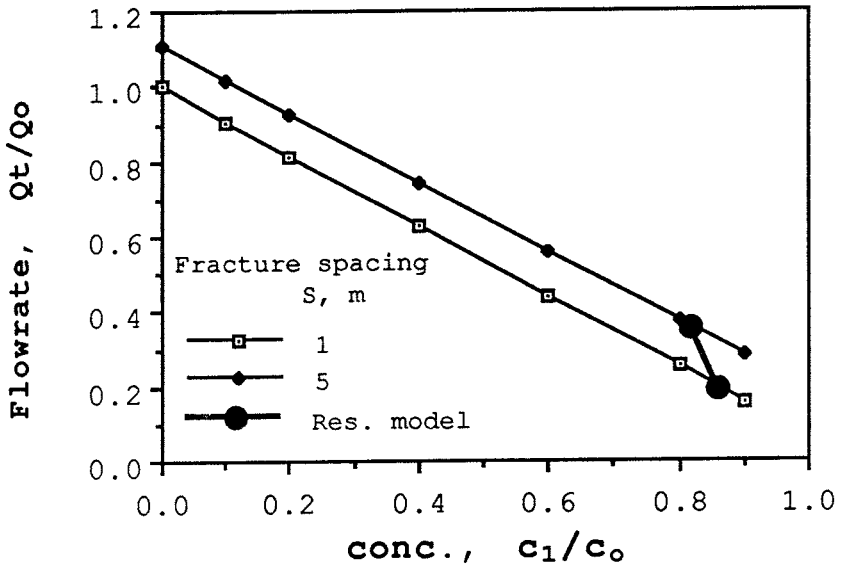

Figure 34. Flow rate dependency on the dimensionless concentration at the mouth of the fracture, for different fracture spacings. $\delta = 0.1$ mm.

The influence of the fracture aperture on the fraction of nuclides which reach the flowing water through the rock (Q_2/Q_t) is also studied. Figure 35 shows that this fraction is increased with the concentration in the fracture and it is smaller for larger fracture apertures. For the reference case this fraction varies from 30 % for zero concentration in the fracture to 60 % for a concentration at the fracture mouth of $0.90 \cdot C_0$.

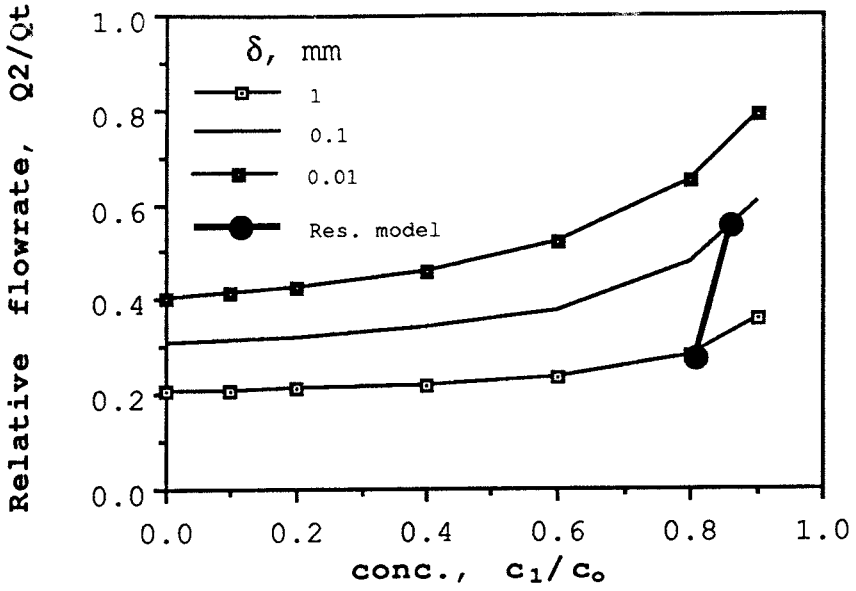

Figure 35. Dependency of the fracture aperture on the fraction of the flow rate through the rock, Q_2. Fracture spacing 1 m.

II.4.1.2 Results for case with plug in the fracture

The fracture was plugged with bentonite. Calculations were performed for a fracture aperture of 0.1 mm, spacings between fractures of 1 m and contact time evaluated at an angle of $\pi/4$. Release for different plug lengths are shown in Figure 36 as a function of the concentration at the fracture mouth. The calculations were performed for a given concentration at the fracture mouth. If the plug length is increased this concentration will be smaller.

Values for the concentration in the fracture are taken from the resistor model and plotted in Figure 36. The thick curve shows as the release changes with the plug length. For example, if there is no plug the concentration at the fracture mouth is about $0.9 \cdot C_0$, and the release is about $0.18 \cdot Q_0$. For a plug length of 10 cm the concentration at the fracture is $0.6 \cdot C_0$ and the release is about $0.12 \cdot Q_0$. This shows that the influence of the plug is not significant, due to the fact that the resistance in the flowing water is more important.

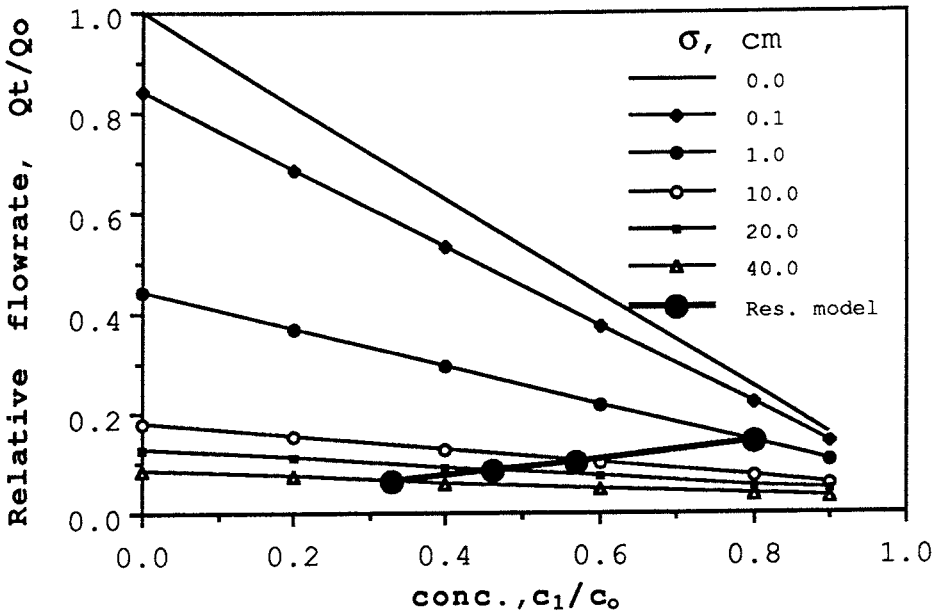

Figure 36. The intersection of the thick line with the curves of flow rate gives the relative equivalent flow rate obtained from concentration at the mouth of the fracture, calculated in the resistor model.

The distribution of the total equivalent flow rate in the different paths (Q_1, Q_2 and Q_3) are modified with the variation of the plug length. Figure 37 shows the fraction of the nuclides which flow only through backfill and bentonite plug in the fracture, Q_1/Q_t. It is observed a strong decrease of this fraction when the plug lengths is increased. The thick curve shows how the release changes with the plug length.

The fraction of nuclide flow rate through the paths Q_2 (see Figure 31) to the total nuclide flow rate (Q_2/Q_t) is strongly increased by effect of the plug. When the plug length is larger, most of the nuclides escape through the rock.

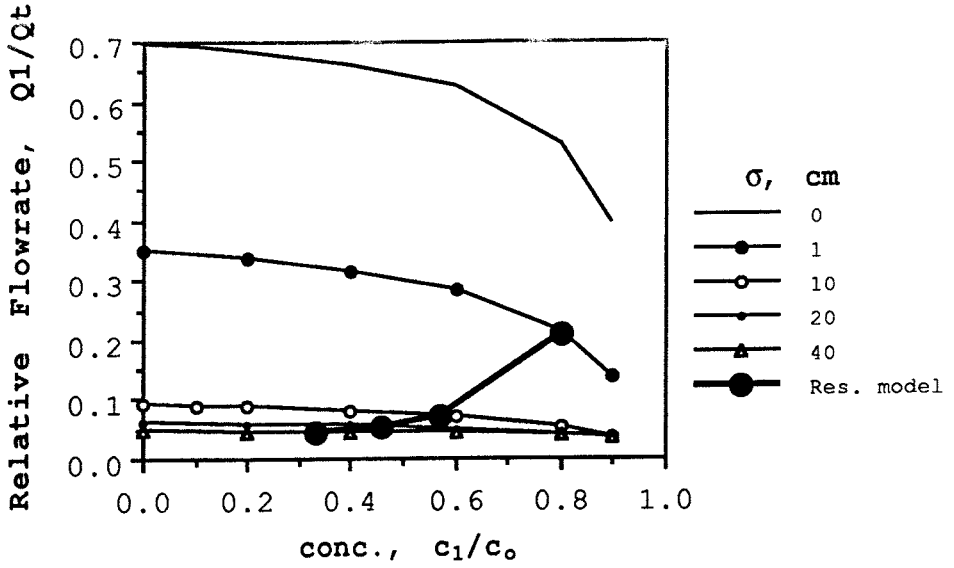

Figure 37. Dependency of the concentration at the fracture mouth on the flow rate through the interface backfill-bentonite, for different plug lengths.

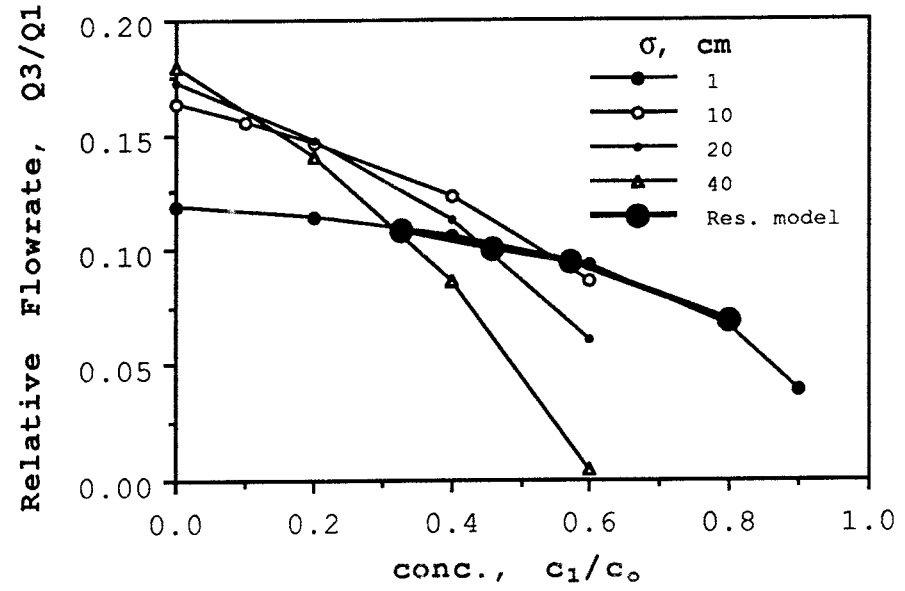

Figure 38. Dependency of the concentration at the fracture mouth on the flow rate through the rock-water interface, for different plug lengths.

The fraction Q_3/Q_t of radionuclides via the path bentonite-rock for different plug lengths is shown in Figure 38. The release of nuclides calculated for concentrations in the fracture taken from the resistor model is almost constant, about 9 % of the total release escape via path Q_3.

II.4.2 Results, 3-D model

The release of radionuclides from the canister, calculated using the 2-D model is dependent of the boundary condition at the mouth of the fracture. We have assumed a certain concentration profile in the fracture. The release of radionuclides may be calculated if the concentration at the mouth of the fracture is known beforehand for a given flow rate of water in the fracture and for a certain plug-length.

To match the resistor model with the release of radionuclides from the canister, we need a reference case, for this reason we have developed a 3-D solution. The release so calculated is considered as the "real" release from the canister. The results of the 3-D model also may be used to compare with the results of the 2-D model.

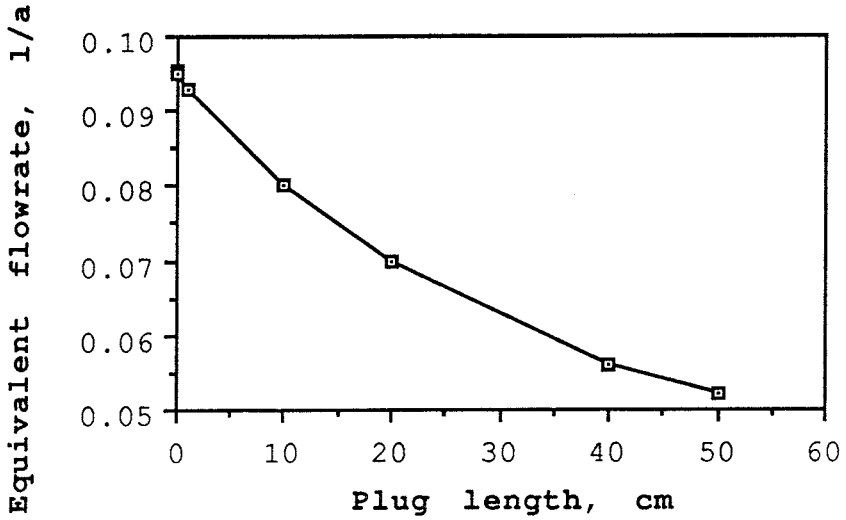

Figure 39. Equivalent flow rate as a function of the plug length. For s=1 m, δ=0.1 mm, and water flux of 0.1 l/m^2·a.

The solution of the 3-D model is very computer time consuming. The typical grid size has been about 20,000 nodes. The model was solved for different

plug lengths, for a fracture spacing of 1 m, a fracture aperture of 0.1 mm and a water flux in the fracture in the z-direction of 0.1 l/m^2.a.

The release of radionuclides from the canister expressed as equivalent flow rate is shown in Figure 39 above. This results indicate that the influence of the plug is not significant. The release is reduced by about a 25 % when the plug length is increased from 0.1 mm (in practice no plug) to 200 mm.

The concentration profile built up in the water flowing around the depository hole, is shown in Figure 40 below. The figure shows small variations in concentration for contact angles between $\pi/2$ and π. The major variation occurs at the inlet of the water-path, for contact-angles less than $\pi/4$.

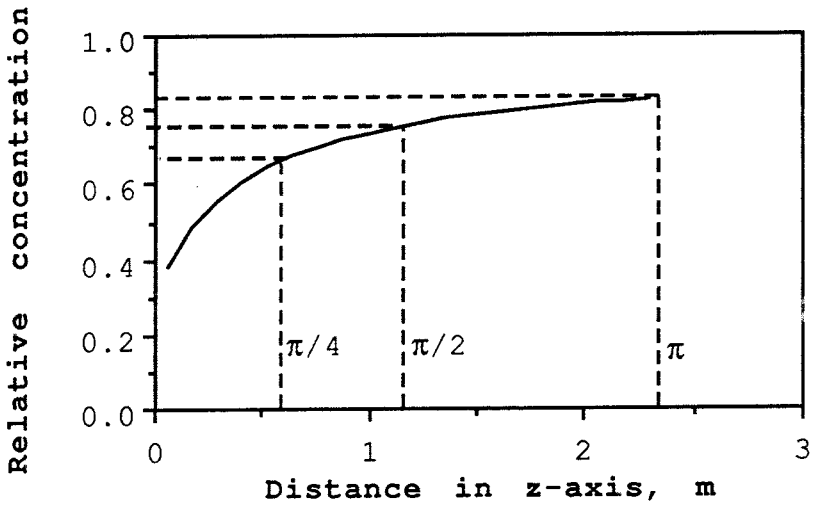

Figure 40. Concentration profile at the interface fracture water - plug. For a plug of 10 cm in length.

The concentration profile at the interfaces bentonite-rock and bentonite-plug (, see Figure 31), is shown in Figure 41. This concentration profile is practically flat with a small and pronounced drop at the vicinity of the fracture mouth. The mean concentration is approximately $0.98 \cdot c_0$.

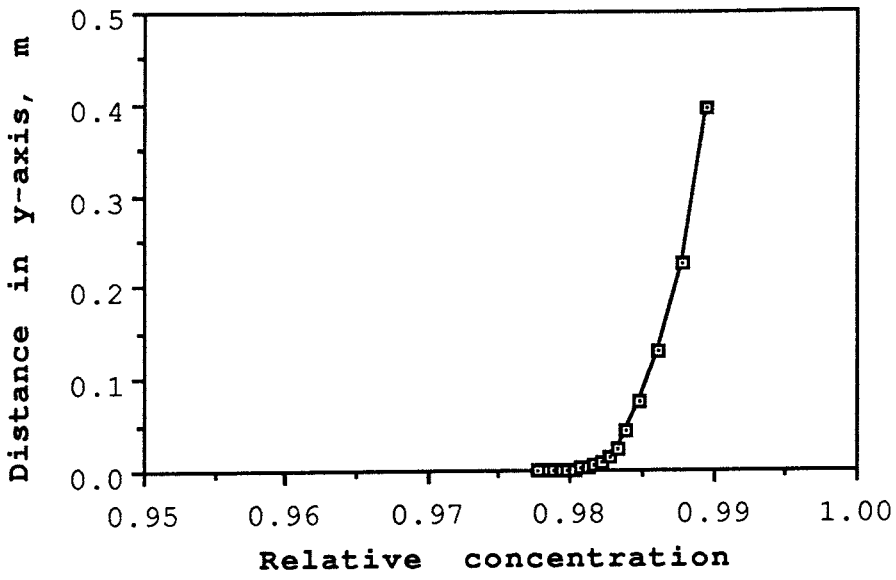

Figure 41. Concentration profile at the interface bentonite - rock. For a plug of 10 cm in length.

Figure 42 shows the concentration profile from the canister surface through the backfill and the bentonite plug into the water in the fracture.

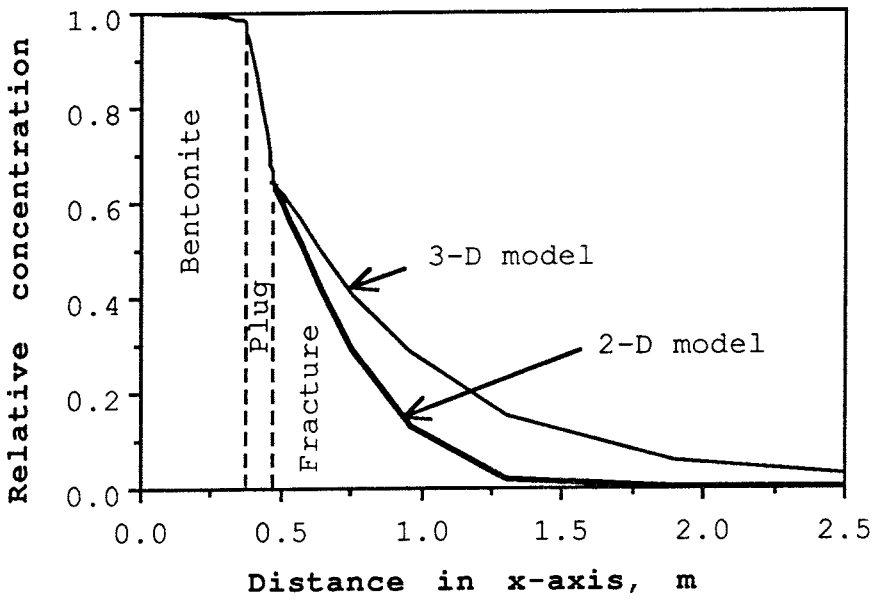

Figure 42. Concentration profile in the different interfaces, at the same level of the fracture. For a plug of 10 cm in length.

A comparison of the results obtained with the 3-D model is made with those obtained in the 2-D model for boundary condition at the mouth of the fracture obtained from the 3-D model. The results are shown in Table 4. The table shows a higher release of radionuclides from the canister by approximately 30 % for the 2-D model. The reason may be that the concentration profile imposed in the fracture in the 2-D model is based solely on the diffusion through the mouth of the fracture and does not account for the diffusion from the rock into and along of the fracture. This can be corroborated by observing in Figure 42 that the concentration profile into the fracture for the 2-D model lies under the curve for the concentration profile obtaining from the 3-D model.

Table 4 Comparison of the total equivalent flow rate calculated by the two numerical models.

		Total equivalent flow rate	
		2-D Model	3-D Model
Plug-length [mm]	c_1/c_o [-]	Q_t' [l/a]	Q_t [l/a]
0.1	0.94	0.135	0.095
10.	0.88	0.127	0.093
100	0.64	0.105	0.080
200	0.53	0.088	0.070

II.5 Conclusion

The results from the numerical solutions of the 2-D and 3-D models do not show a clear and large difference in the magnitude of the equivalent flow rate of radionuclides whether a clay plug is introduced into the fracture or not. It was found that the release is decreased by a factor of 1.5 to 2 when the plug length increases from 0 to 50 cm.

Changes in the conditions in the system studied (changes in aperture, spacing, plug-length, etc) not only affects the total equivalent flow rate, it also changes the distribution of the equivalent flow rates between the different flow paths.

It is observed that the release of radionuclides obtained from the 2-D model with respect to the 3-D model is overestimated by about 30%. This difference arises as was shown, because the concentration profile imposed within the fracture does not account for the contribution to this profile from the lateral diffusion from the ceiling and floor of the fracture.

List of SKB reports

Annual Reports

1977-78
TR 121
KBS Technical Reports 1 – 120
Summaries
Stockholm, May 1979

1979
TR 79-28
The KBS Annual Report 1979
KBS Technical Reports 79-01 – 79-27
Summaries
Stockholm, March 1980

1980
TR 80-26
The KBS Annual Report 1980
KBS Technical Reports 80-01 – 80-25
Summaries
Stockholm, March 1981

1981
TR 81-17
The KBS Annual Report 1981
KBS Technical Reports 81-01 – 81-16
Summaries
Stockholm, April 1982

1982
TR 82-28
The KBS Annual Report 1982
KBS Technical Reports 82-01 – 82-27
Summaries
Stockholm, July 1983

1983
TR 83-77
The KBS Annual Report 1983
KBS Technical Reports 83-01 – 83-76
Summaries
Stockholm, June 1984

1984
TR 85-01
Annual Research and Development Report 1984
Including Summaries of Technical Reports Issued during 1984. (Technical Reports 84-01 – 84-19)
Stockholm, June 1985

1985
TR 85-20
Annual Research and Development Report 1985
Including Summaries of Technical Reports Issued during 1985. (Technical Reports 85-01 – 85-19)
Stockholm, May 1986

1986
TR 86-31
SKB Annual Report 1986
Including Summaries of Technical Reports Issued during 1986
Stockholm, May 1987

1987
TR 87-33
SKB Annual Report 1987
Including Summaries of Technical Reports Issued during 1987
Stockholm, May 1988

1988
TR 88-32
SKB Annual Report 1988
Including Summaries of Technical Reports Issued during 1988
Stockholm, May 1989

1989
TR 89-40
SKB Annual Report 1989
Including Summaries of Technical Reports Issued during 1989
Stockholm, May 1990

Technical Reports

List of SKB Technical Reports 1991

TR 91-01
Description of geological data in SKB's database GEOTAB Version 2
Stefan Sehlstedt, Tomas Stark
SGAB, Luleå
January 1991

TR 91-02
Description of geophysical data in SKB database GEOTAB Version 2
Stefan Sehlstedt
SGAB, Luleå
January 1991

TR 91-03
1. The application of PIE techniques to the study of the corrosion of spent oxide fuel in deep-rock ground waters
2. Spent fuel degradation
R S Forsyth
Studsvik Nuclear
January 1991

TR 91-04
Plutonium solubilities
I Puigdomènech[1], J Bruno[2]
[1]Enviromental Services, Studsvik Nuclear, Nyköping, Sweden
[2]MBT Tecnologia Ambiental, CENT, Cerdanyola, Spain
February 1991

TR 91-05
Description of tracer data in the SKB database GEOTAB
SGAB, Luleå
April, 1991

TR 91-06
Description of background data in the SKB database GEOTAB Version 2
Ebbe Eriksson, Stefan Sehlstedt
SGAB, Luleå
March 1991

TR 91-07
Description of hydrogeological data in the SKB's database GEOTAB Version 2
Margareta Gerlach[1], Bengt Gentzschein[2]
[1]SGAB, Luleå
[2]SGAB, Uppsala
April 1991

TR 91-08
Overview of geologic and geohydrologic conditions at the Finnsjön site and its surroundings
Kaj Ahlbom[1], Sven Tirén[2]
[1]Conterra AB
[2]Sveriges Geologiska AB
January 1991

TR 91-09
Long term sampling and measuring program. Joint report for 1987, 1988 and 1989. Within the project: Fallout studies in the Gideå and Finnsjö areas after the Chernobyl accident in 1986
Thomas Ittner
SGAB, Uppsala
December 1990

TR 91-10
Sealing of rock joints by induced calcite precipitation. A case study from Bergeforsen hydro power plant
Eva Hakami[1], Anders Ekstav[2], Ulf Qvarfort[2]
[1]Vattenfall HydroPower AB
[2]Golder Geosystem AB
January 1991

TR 91-11
Impact from the disturbed zone on nuclide migration – a radioactive waste repository study
Akke Bengtsson[1], Bertil Grundfelt[1], Anders Markström[1], Anders Rasmuson[2]
[1]KEMAKTA Konsult AB
[2]Chalmers Institute of Technology
January 1991

TR 91-12
Numerical groundwater flow calculations at the Finnsjön site
Björn Lindbom, Anders Boghammar, Hans Lindberg, Jan Bjelkås
KEMAKTA Consultants Co, Stockholm
February 1991

TR 91-13
Discrete fracture modelling of the Finnsjön rock mass Phase 1 feasibility study
J E Geier, C-L Axelsson
Golder Geosystem AB, Uppsala
March 1991

TR 91-14
Channel widths
Kai Palmqvist, Marianne Lindström
BERGAB-Berggeologiska Undersökningar AB
February 1991

TR 91-15
Uraninite alteration in an oxidizing environment and its relevance to the disposal of spent nuclear fuel
Robert Finch, Rodney Ewing
Department of Geology, University of New Mexico
December 1990

TR 91-16
Porosity, sorption and diffusivity data compiled for the SKB 91 study
Fredrik Brandberg, Kristina Skagius
Kemakta Consultants Co, Stockholm
April 1991

TR 91-17
Seismically deformed sediments in the Lansjärv area, Northern Sweden
Robert Lagerbäck
May 1991

TR 91-18
Numerical inversion of Laplace transforms using integration and convergence acceleration
Sven-Åke Gustafson
Rogaland University, Stavanger, Norway
May 1991

TR 91-19
NEAR21 - A near field radionuclide migration code for use with the PROPER package
Sven Norman[1], Nils Kjellbert[2]
[1]Starprog AB
[2]SKB AB
April 1991

TR 91-20
Äspö Hard Rock Laboratory. Overview of the investigations 1986-1990
R Stanfors, M Erlström, I Markström
June 1991

TR 91-21
Äspö Hard Rock Laboratory. Field investigation methodology and instruments used in the pre-investigation phase, 1986-1990
K-E Almén, O Zellman
June 1991

TR 91-22
Äspö Hard Rock Laboratory. Evaluation and conceptual modelling based on the pre-investigations 1986-1990
P Wikberg, G Gustafson, I Rhén, R Stanfors
June 1991

TR 91-23
Äspö Hard Rock Laboratory. Predictions prior to excavation and the process of their validation
Gunnar Gustafson, Magnus Liedholm, Ingvar Rhén, Roy Stanfors, Peter Wikberg
June 1991

TR 91-24
Hydrogeological conditions in the Finnsjön area. Compilation of data and conceptual model
Jan-Erik Andersson, Rune Nordqvist, Göran Nyberg, John Smellie, Sven Tirén
February 1991

TR 91-25
The role of the disturbed rock zone in radioactive waste repository safety and performance assessment. A topical discussion and international overview.
Anders Winberg
June 1991

TR 91-26
Testing of parameter averaging techniques for far-field migration calculations using FARF31 with varying velocity.
Akke Bengtsson[1], Anders Boghammar[1], Bertil Grundfelt[1], Anders Rasmuson[2]
[1]KEMAKTA Consultants Co
[2]Chalmers Institute of Technology

TR 91-27
Verification of HYDRASTAR. A code for stochastic continuum simulation of groundwater flow
Sven Norman
Starprog AB
July 1991

TR 91-28
Radionuclide content in surface and groundwater transformed into breakthrough curves. A Chernobyl fallout study in an forested area in Northern Sweden
Thomas Ittner, Erik Gustafsson, Rune Nordqvist
SGAB, Uppsala
June 1991

TR 91-29
Soil map, area and volume calculations in Orrmyrberget catchment basin at Gideå, Northern Sweden
Thomas Ittner, P-T Tammela, Erik Gustafsson
SGAB, Uppsala
June 1991